

ΠΑΝΕΠΙΣΤΗΜΙΟ ΘΕΣΣΑΛΙΑΣ

M.Sc. Thesis

EXERGY ANALYSIS AND OPTIMIZATION OF THE POWER MODE OPERATION OF A
BIMODAL NUCLEAR THERMAL ROCKET.

Εξεργειακή ανάλυση και βελτιστοποίηση ενεργειακής λειτουργίας ενός 2-λειτουργικού θερμικού
πυρηνικού πυραύλου.

Μεταπτυχιακή Εργασία

3μελής επιτροπή:

1^{ος} εξεταστής: Αναστάσιος Σταμάτης Αναπληρωτής Καθηγητής

2^{ος} εξεταστής: Γεώργιος Λυμπερόπουλος Καθηγητής

3^{ος} εξεταστής: Νικόλαος Ανδρίτσος Καθηγητής

Σκορδίλης Ερωτόκριτος

25/2/2013

EXERGY ANALYSIS AND OPTIMIZATION OF THE POWER MODE OPERATION OF A
BIMODAL NUCLEAR THERMAL ROCKET

By

Erotokritos Skordilis

Graduate of Computer and Communication Engineering Department, University of Thessaly 2011

Thesis submitted to the Faculty of the Graduate School of the University of Thessaly, Department of
Mechanical Engineering, in partial fulfillment of the requirements for the degree of Master of Applied
Science

2012

© Copyright by Erotokritos Skordilis 2012

DEDICATION

To my family...

ACKNOWLEDGEMENTS

This thesis would have been impossible to become reality without the continuous support and guidance of my advisor, Professor Anastasios Stamatis, for the whole duration of my postgraduate studies at the Mechanical Engineering Department of the University of Thessaly. Furthermore, I would like to thank professors G. Saharidis, A. Ziliaskopoulos, N. Pelekasis and G. Liberopoulos, for introducing me to the vast academic area of mechanical engineering during the last one and a half years.

It would have been inappropriate, of course, not to mention my colleagues and best friends M. Ioanniti, K. Pavlou and El. Benos with whom we started the project of the exergy analysis on a Bimodal Nuclear Thermal Rocket as a research paper and to thank them for their immense help and guidance to the fascinating paths of Thermodynamics. Without their support this thesis would not have reached the point that it is now.

On a more personal note, I would like to thank all of my close friends that tolerated my erratic and sometimes bothersome behavior during my time as a postgraduate student. They have been my mental support and they have kept me grounded for the past several years.

This thesis is also dedicated to my best friends from school, Th. Liakouras, D. Douvitsas and K. Fronimos, with whom we shared many experiences, both good and bad, and I am deeply grateful of our strong and everlasting friendship.

Finally, I would like to thank my family for their continuous and perpetual support both economically and mentally all these nine years as a student. Their endless guidance and consultation has been an endlessly limpid beacon and for that I thank them very much.

TABLE OF CONTENTS

Nomenclature.....	8
List of Figures.....	10
Chapter 1	
Introduction.....	11
1.1 Nuclear Thermal Propulsion.....	12
1.1.1 Nuclear Fission as a Power Source.....	12
1.1.2 Bimodal Nuclear Thermal Rocket.....	13
1.2 Project Overview.....	14
1.2.1 Motivation & Objective.....	14
1.2.2 Approach.....	14
1.2.3 Contribution.....	15
Chapter 2	
2.1 Nuclear Fission Basics.....	16
2.2 History of Nuclear Propulsion.....	19
2.2.1 Project Rover.....	19
2.2.2 NERVA: Nuclear Engine for Rocket Vehicle Application.....	20
2.2.3 Nuclear Thermal Rockets.....	22
2.2.4 Termination of NERVA Program.....	24
2.3 Modern Nuclear Thermal Rocket Concepts.....	25
2.3.1 Project Prometheus.....	25
2.3.2 Project Bifrost.....	25
2.4 Future of Nuclear Propulsion and other Advanced Projects.....	26
Chapter 3	
3.1 Brayton Power Systems using Nuclear Reactors.....	28
3.2 Engine System.....	28
3.3 Ideal and Non-Ideal Brayton Cycles.....	29
3.3.1 Ideal Brayton Cycle.....	30
3.3.2 Non-Ideal Brayton Cycle.....	32
3.3.3 Brayton Cycle of the Bimodal Nuclear Thermal Rocket.....	33
Chapter 4	
4.1 Exergy.....	38
4.2 Exergy Analysis.....	39
4.3 BNTR Closed Brayton Cycle Exergy Analysis.....	39

4.4 Works, Exergy Destruction and Exergy Efficiency.....	40
Chapter 5	
5.1 Finite Time Thermodynamics.....	42
5.1.1 Introduction to Finite Time Thermodynamics.....	42
5.1.2 Optimization of the other heat-engine cycles.....	43
5.1.3 Power Density Analysis of the closed Brayton cycle.....	44
Chapter 6	
Results.....	54
Conclusions.....	62
Annex.....	63
References.....	68

NOMENCLATURE

^{235}U	Isotope 235 of Uranium
^{239}Pu	Isotope 239 of Plutonium
\dot{W}_{out}	Work output of the cycle
\dot{Q}_{in}	Input heat transfer
r_p	Pressure ratio (ideal Brayton cycle)
e_R	Recuperator efficiency
T_i	Temperature of i_{th} state
h_i	Enthalpy of i_{th} state
\dot{W}_t	Work output of the turbine
\dot{W}_c	Work output of the compressor
\dot{m}	Mass flow
P_i	Pressure of i_{th} state
Pr_c	Pressure ratio of the compressor
Pr_t	Pressure ratio of the turbine
UA	Heat conductance coefficient of the recuperator
UA_H	Heat conductance coefficient of the reactor
UA_L	Heat conductance coefficient of the heat pipe manifold
C_p	Specific heat capacity at constant temperature
$Ph_{ex,i}$	Physical exergy of i_{th} state
S_i	Entropy of i_{th} state
$Ch_{ex,i}$	Chemical exergy of i_{th} state
x_{He}	Percentage of Helium
x_{Xe}	Percentage of Helium
R_{He_Xe}	Ideal gas constant for He/Xe mixture
Ex_{total_i}	Total exergy of i_{th} state
$P_{compressor}$	Work output of the compressor
$P_{turbine}$	Work output of the turbine
P_{total}	Work output of the alternator (total output of the cycle)
Δh	Enthalpy drop
$Ex_destruction_j$	Exergy destruction at j_{th} component
T_H	Temperature at hot thermal reservoir

T_L	Temperature at cold thermal reservoir
COP_{ref}	Coefficient of performance for refrigeration
COP_{hp}	Coefficient of performance for heat pumps
D_i	Pressure drop in i_{th} duct
C_{wf}	Thermal capacity rate of working fluid
Q_H	Rate of heat transferred from heat source to working fluid
Q_L	Rate of heat rejected from working fluid to heat source
Q_R	Heat regenerated in regenerator
E_H	Effectiveness of hot-side heat exchanger
E_L	Effectiveness of cold-side heat exchanger
E_R	Effectiveness of regenerator
N_H	# of heat transfer units of hot-side exchanger
N_L	# of heat transfer units of cold-side exchanger
N_R	# of heat transfer units of regenerator
\bar{W}	Dimensionless power output
\bar{P}	Power density
\bar{P}_{dens}	Dimensionless Power density
u_H	Heat conductance distribution of hot-side heat exchanger
u_L	Heat conductance distribution of cold-side heat exchanger

Greek Symbols

η_{th}	Thermal efficiency of ideal Brayton cycle
η_t	Efficiency of turbine
η_c	Efficiency of compressor
η_{alt}	Efficiency of the alternator
η_{exergy_j}	Exergy efficiency at j_{th} component
γ	Specific heat capacity C_p/C_v
τ	T_H/T_L ratio

LIST OF FIGURES

Figure 1: NERVA-type fuel bar

Figure 2: Cross section of neutron interactions

Figure 3: Project Rover nuclear rocket engines

Figure 4: Phoebus-2A nuclear reactor

Figure 5: Kiwi nuclear reactor

Figure 6: JIMO

Figure 7: BNTR engine system

Figure 8: Ideal closed Brayton cycle/T-s diagram

Figure 9: Non-ideal closed Brayton cycle (recuperated)/T-s diagram

Figure 10: Closed Brayton cycle on a BNTR

Figure 11: T-s diagram of an irreversible regenerated Brayton cycle

Chapter 1

Introduction

Since the last Moon landing, over 40 years have passed and many people have been disappointed with the lack of progress in continuing the Apollo journey. To address this, and the apparent lack of direction with NASA, the U.S. Government launched the Vision for Space Exploration (VSE), an initiative under the leadership of former President Bush. This plan set out a 2020 timetable for the return of humans back to the Moon and by 2024 the plan was to have a permanent human settlement [1]. The most exciting aspect of the Vision, however, is the planning of landing humans on Mars by the year 2030. In order for that to happen new means for power and propulsion have to be developed, more powerful than current chemical propulsion elements. The most promising power source contemporarily is nuclear fission so it is pellucid that VSE lists nuclear propulsion and power research as “key to enabling other advanced robotic missions and human missions beyond Earth’s orbit” [2]. Since then many studies conducted by various researchers identified nuclear propulsion and power as a key element for space crafts to go beyond Low Earth Orbit and embark to exploration of the Solar System.

Nuclear fission in the form of nuclear thermal propulsion provides twice the fuel efficiency of chemical propulsion, which can lead to lighter and less expensive vehicles, because of the lower fuel/oxidizer mass ratio. A second and very important feature of the nuclear thermal propulsion is that the spacecraft’s power system utilizes the same nuclear reactor as the propulsion system, which can provide consistent electric power regardless of distance from the Sun, thus reducing the weight of a separate, independent power system. For these reasons, a system which uses a common reactor for propulsion and power generation, formally known as a Bimodal Nuclear Thermal Rocket system, is the most suitable engine for manned Mars exploration.

The main purpose of this thesis is the exergy analysis and optimization of the power system on a Bimodal Nuclear Thermal Rocket. Most of the material used as input was taken from Joshua Clough’s doctoral dissertation “Integrated Propulsion and Power Modeling for Bimodal Nuclear Thermal Rocket”. In his dissertation there is, as can be seen by the title, both propulsion and power modeling, however our purpose is directed only in the extension of the power modeling, thus introducing an exergy analysis and optimization for the spacecraft’s power generation.

1.1 Nuclear Thermal Propulsion

1.1.1 Nuclear Fission as a Power Source

Making interplanetary travel time practicable for manned and unmanned missions means new propulsion systems and new ways of generating power must be explored.

Perhaps, after the accidents on Three Mile Island and Chernobyl, or the more recent at Fukushima, the idea of using nuclear energy to propel and power a spacecraft means great risk, of possible radiation hazard, to many people. Fortunately, there is a substantial amount of people that, at nuclear energy, see a big opportunity to free up the Solar System to not only to robotic but also to human interplanetary missions. This is normal since the energy obtained by nuclear reactions is of the order of million times greater than that from a typical chemical reaction.

In fission the nuclei of atoms of properly chosen materials (e.g. ^{235}U and ^{239}Pu) are broken apart by neutrons. The neutrons needed are produced by these materials, but their fissioning effect becomes efficient only when a 'critical' mass of material is assembled. Using the electronvolt (eV) as energy unit, fissioning ^{235}U yields 160 MeV per fission fragment, to be compared to a fraction of an electronvolt in chemical combustion. In more common units, fission heat release per unit propellant mass, J , is vastly larger than of H_2 / O_2 propellants in a rocket (about $1.35 \times 10^7 \text{ J / kg}$). In fact, as any energy release process, nuclear reactions convert fuel mass into energy according to the famous Einstein equation $E = mc^2$. The energy per unit mass, J , available in fission is of the order of 8.2×10^{13} using ^{235}U , almost 10^7 times larger than in chemical combustion.

Nuclear fission has been used for decades for propulsion and power generation in naval systems, especially from both USA and Russia (former USSR). Their respective fleets had and continue to have numerous vessels, ranging from ballistic missile submarines to aircraft carriers, driven by nuclear fission reactors, not very different than that considered for space propulsion and power generation. In USA there was also a thought back in the 60's (programs NEPA and ANP) to develop a nuclear powered bomber, which would had unlimited range of operation, but putting a nuclear reactor on an airplane in case it suddenly crashes near a populated area was considered to be extremely risky so this plan abandoned few years later. Similar thoughts had been at USSR also (Tupolev prototype Tu-119). Judging from the success nuclear power has on navy vessels, there is no doubt that with proper design and development and especially with the political and economic support, a new generation of space propulsion and power generation systems can be developed which will push spacecrafts well beyond LEO, making manned interplanetary missions a reality and thus introducing new borders for human exploration of the Solar System.

Fundamental physics tells us that the only non-chemical source of energy for space propulsion and power generation is nuclear. Nuclear fission has been tested since the 1950's.

Fission can meet the two ideal requirements of lowering propellant consumption while still keeping thrust reasonable, that is, comparable to that of conventional rockets. It is this multiple capability, independence from propellant, large specific impulse and large power in a compact package, that suggests nuclear propulsion as the only practicable means of reaching the planets of our Solar System.

1.1.2 Bimodal Nuclear Thermal Rocket

During the course of a typical NTR-powered mission to Mars (the “next big thing” in space exploration), thrust is generated for only one hour. For the remainder of the mission, the reactor is idle, producing radioactive decay heat that must be exhausted from the system. Bimodal Nuclear Thermal Rocket (BNTR) systems operate the nuclear reactor in two ways: a high-power propulsion mode and a secondary, low-power, power generation mode. The two-way usage of the reactor plays a significant role since there is not the need for multiple reactors, solar sails or other systems, thus reducing the total mass of the rocket very much. Such a weight loss is a big advantage for future space travel, since more payload than propellant can be transferred in orbit.

The so-called nuclear thermal rocket (NTR), one of the many propulsion systems based on fission, is essentially a miniature nuclear power station, where solid ^{235}U - enriched fuel fissions, release heat to a coolant fluid which plays also the role of propellant. This fluid may be exhausted as in conventional rocket, or used in a thermodynamic cycle to produce electric power.

A BNTR power system uses the propulsion reactor as a heat source (in other words as a furnace) and connects it to a separate closed-loop power cycle. This closed-loop will use an inert gas (in our case a He-Xe mixture) instead of hydrogen, which is used in the propulsion mode, in order to prevent reactor corrosion. In this system, the power cycle coolant passes through reactor support elements called ‘tie-tubes’, which are showed in Figure 1.

What is derived from the above, the primary objective of the BNTR power system is to provide electric power at the highest conversion efficiency possible, while also providing sufficient reactor cooling. This leads to a trade-off between pressure loss and heat transfer within the tie tube elements. The efficiency of a closed loop power cycle will decrease with increasing pressure loss. The available input heat and reactor cooling increase with the rate of heat transfer. The goals of high heat transfer and low pressure drop must be examined together because optimizing for one tends to minimize the other. For example, heat transfer can be improved by increasing flow rate. Doing so, however, also increases the pressure loss. As such, the trade-off between heat transfer and pressure loss will drive the power system design and analysis.

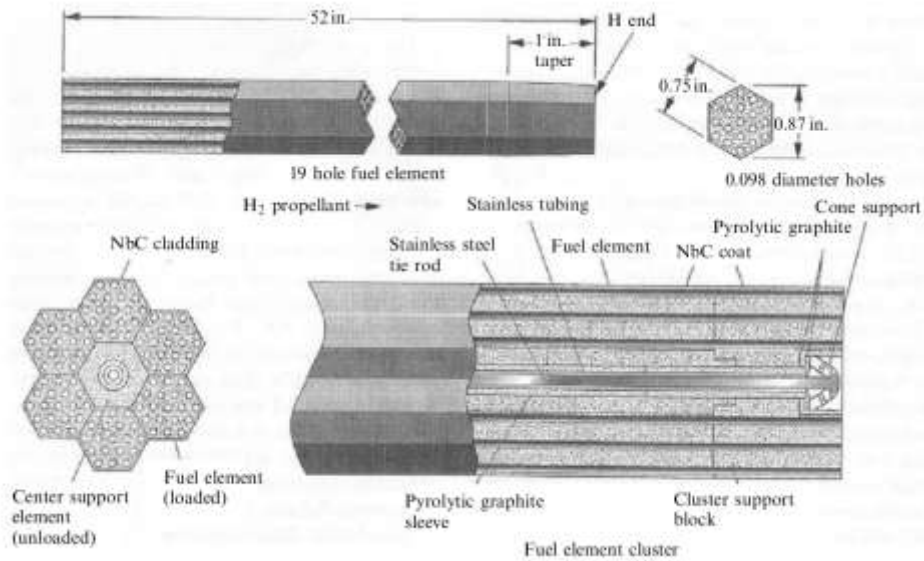


Figure 1: Structure and size of a NERVA-type fuel bar.

1.2 Project Overview

1.2.1 Motivation & Objective

This work has begun as a research project for the postgraduate course “Thermal Systems Design”, conducted by Associate Professor A. Stamatis, who is also the supervisor of this thesis. Along with the dear and respected colleagues Ioanniti M., Benos El. and Pavlou K., a first approach of a thermodynamics and exergy analysis for a BNTR’s power system was introduced, though it contained some compromises that they are dealt with in this thesis.

The objective of this thesis is the exergy analysis and optimization of a BNTR’s power system. During the research regarding the power production at nuclear powered space vehicles and stations, a wealth of information and studies revealed the extended work done by many researchers around the world either at universities or space agencies (NASA, ESA, RSA etc.) However, there was virtually no research considering thermodynamics and exergy analysis and optimization, thus leaving a gap to this area. It is unclear why this happened, but if the BNTR is to be utilized in the near future, then the scope of this thesis is to demonstrate a solid approach to exergy analysis and optimization of such systems, in order to lead other researchers to other implementations regarding this.

1.2.2 Approach

The basic approach of this thesis’ research is to create a BNTR power system model through the creation of a numerical code, which provides sufficient results regarding the various properties concerned with the exergy analysis and optimization. These properties

represent values such as entropy, enthalpy, turbine and compressor pressure ratios among others (all properties are listed under the *nomenclature* section).

The model describes entirely the closed Brayton cycle from a component-level operation, where each of the components is presented along with each of the components properties. More specifically, the entire Brayton cycle was separated into different sections, where each section represents a state. At these states, calculations in order to determine properties such as pressure, temperature, enthalpy, entropy and physical and chemical exergies were conducted. These properties will be then used for determining the total output of the power system. After that, a first approach of an exergy optimization is introduced. This attempt to optimize the closed Brayton cycle under consideration will extrapolate its results from the point of the power density analysis.

The modeling was performed using the Mathworks MATLAB 7.12 R2011a Simulation tool. No further sub-packages were used for the calculation of specific variables, such as entropy, enthalpy and chemical exergies. The model was utilized on an Intel Core2Duo E6600 2.4 GHz processor, aimed by 4GB RAM.

1.2.3 Contribution

The primary contribution of this thesis is, hopefully, a first-of-its-kind model and analysis of a BNTR power mode system. This study aims to produce exergy analysis and optimization for a closed Brayton cycle, which uses a nuclear reactor as a heat capacitor. The results are the first of their kind and hopefully represent a decent approach to the power operation of a Bimodal Nuclear Thermal Rocket. It is prudent to state that the results obtained from this thesis can be used for future studies concerning the power production on a Bimodal Nuclear Thermal Rocket, which will hopefully lead to better and better results each time.

Chapter 2

2.1 Nuclear Fission Basics

Nuclear fission was discovered in Germany, by Hahn and Strassmann in 1939, but it was in the United States that the first controlled release of fission energy was established by Fermi and colleagues in 1942. The first nuclear reactor was built in a squash court at the University of Chicago. The essential process is the absorption of a neutron by a uranium nucleus, which causes the nucleus to split into two nuclei, with the release of just under 200MeV of energy. Most of this is in the form of kinetic energy in the two fission fragments, with a smaller fraction released in gamma-rays. The importance of fission in uranium is that two or more neutrons are emitted at the same time as the fission of the nucleus occurs. In principle, these neutrons can go on to interact with another uranium nucleus and cause that to split. In this way, a chain reaction can be set up with more and more nuclei undergoing fission and more and more neutrons being released to cause yet more fission. Since the rate at which energy is released depends only on the neutron flux, the power output of such a system can be controlled by inserting materials that absorb neutrons. This is the nuclear reactor used to power electricity generation and it also forms the basics of a nuclear rocket engine.

The energy released in the fission-fragment velocity is very quickly converted into heat as the fragments slow down in the uranium, thus leading uranium during controlled nuclear fission to become very hot (in fact the theoretical limit to the temperature that could be reached is very high indeed). The uranium would melt well before this limit. Because of that, once fission energy is being released, the process of making use of this energy is simply that of cooling the uranium and using the heat extracted to provide power. For the generation of electricity, this can be by any conventional means: some reactors use water as a coolant, which is converted to steam, to use in a turbine driving a generator. Others use gas (CO_2), or a liquid metal like sodium, to cool the uranium and carry the heat out of the reactor to power a steam generation system.

Uranium is a natural material and has properties which make the whole process much more complicated than the simple idea outlined above. There are two main isotopes found in natural uranium: ^{235}U , which is the majority constituent, and ^{238}U , which forms just 0.72% of the total. Although ^{238}U undergoes fission, it is the properties of the much rarer ^{235}U that dominate the process. This is because of the complex way neutrons interact with these heavy nuclei. In addition to causing fission, a neutron can be scattered, elastically or inelastically, or it can be absorbed without causing fission. The probability of these different interactions depends on the energy of the neutron and which isotope it encounters as it scatters through the uranium. The probabilities of these different processes are expressed as cross-sections (Figure 2)

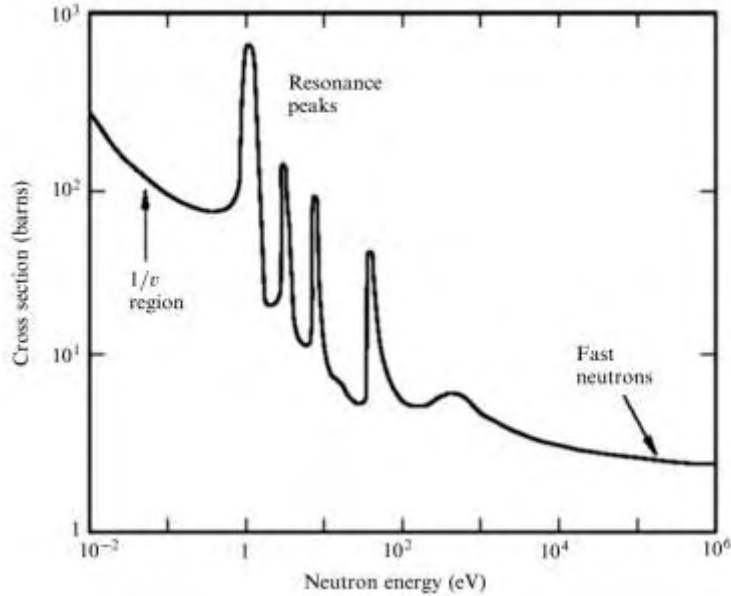


Figure 2: Schematic graph of the cross-section for neutron interactions

^{238}U is capable of fission, but the probability is low, and falls to zero for incident neutrons with energy less than about 1.5MeV. The inelastic scattering quickly slows the neutrons down to less than this energy and thereafter they cannot cause fission in ^{238}U . Neutrons of any energy can cause fission in ^{235}U with significantly higher probability. The probability increases rapidly as the neutron energy decreases, and reaches a value some 1000 times higher than for ^{238}U at very low neutron energies. Low-energy neutrons are described as “thermal” because their kinetic energy, which is much less than 1eV, is close to that of the thermal motion of the atoms in the uranium matrix. Neutrons only interact with the nucleus, because they have no electric charge, so they can remain free in the matrix, at thermal energies. Inelastic scattering will gradually reduce the energy of the fission neutrons from 200MeV down to fractions of an electronvolt. Therefore, they can induce fission in ^{235}U with high probability.

The problem with natural uranium is twofold: the ^{235}U encounters are rare (approx. 0.72%), so the product of cross-section and encounter probability is rather small. Resonance absorption occurs in ^{238}U , where the probability of loss of the neutron is very high at one of a band of different intermediate energies. Neutrons losing energy by inelastic scattering in the matrix must pass through this range of energies, where absorption and loss have a very high probability. This means that in natural uranium, which is mostly consists of ^{238}U , very few of the fission neutrons survive down to thermal energies, where they can cause fission in the rare ^{235}U nuclei. It is not possible to sustain a chain reaction in pure natural uranium.

There are two approaches that can improve the chances for a sustainable reaction. The first and obvious route is to increase the percentage of ^{235}U in the matrix. This simply raises the probability of an interaction between a cooling fission neutron and a ^{235}U nucleus, until the

reaction becomes self-sustaining. Uranium, with enough ^{235}U in it to sustain a chain reaction, is called “enriched”, and depending on the intended use, can have 2%, 20%, 50% or even 90% of ^{235}U . The process of enrichment is complicated and costly, since the atoms are only distinguishable by their atomic mass and not charge or chemical nature. Methods, which preferentially select the lighter isotope, are based on diffusion of a gaseous compound of the metal, usually uranium hexafluoride, through filters, or in centrifuge.

The second approach is to attempt to slow the neutrons down quickly. So that they reach thermal energies without being lost by resonance absorption in the ^{238}U . This process involves a “moderator”, usually carbon or water, that is very good at slowing the neutrons by inelastic scattering and, at the same time, does not absorb them. The moderator can be mixed intimately with the uranium atoms, in a homogeneous reactor, or the uranium and moderator can be in separate blocks, the heterogeneous reactor. The latter is more effective in sustaining the chain reaction with uranium of low enrichment and it can even allow the use of natural uranium. In the homogeneous reactor, the neutrons simply have more collisions with moderator nuclei than with ^{238}U nuclei, so the probability of loss is reduced. In the heterogeneous reactor, a further improvement in the reaction takes place. The uranium is in separate blocks (typically cylindrical rods), separated by blocks of moderator. Cooling neutrons in the energy range where resonance absorption occurs, cannot detect every uranium atom in the reactor. They cannot penetrate very deeply into the fuel rod because they are absorbed in the first few millimeters. The neutrons that penetrate to the central region are exclusively those that cannot be lost to resonance absorption, but can cause fission in the relatively rare ^{235}U nuclei. This means that more ^{238}U can be included in the reactor, without the corresponding loss of neutrons. It is thus possible to build a reactor containing exclusively natural uranium, using the heterogeneous system. This is the system that is used for most nuclear power stations. To sustain a chain reaction in pure uranium requires it to be highly enriched, perhaps more than 90% ^{235}U . Progressive use of moderator allows the use of lower enrichment down to natural uranium. It will perhaps be obvious that the size of the reactor increases, as more “moderator” is used. It is size, more than anything else, which is the critical parameter for space reactors, whether they are to be used to generate electricity or as rocket engines. The need to keep the reactor dimensions small will require the use of enriched uranium. Plutonium can be used in the same way as enriched uranium, but it is so poisonous and radioactive, that safety issues would add considerably to the complexity of a reactor that had to be launched.

2.2 History of Nuclear Propulsion

2.2.1 Project Rover

Because of the need for carrying the heavy atomic and thermonuclear bombs of the late 1940s, the great geopolitical powers of the era, the USA and the Soviet Union, explored the possibility of nuclear propulsion from the late 1940s throughout the 1950s and until the early 1990s. In the United States, the reason for starting the development of nuclear propulsion by the Atomic Energy Commission (i.e. AEC) in 1953 (through the ROVER program) was the perceived necessity for a 75,000lb_f thrust nuclear thermal rocket to power the third stage of the US intercontinental ballistic missiles (ICBM). In 1956 the United States Air Force joined ROVER, but after the test flight of Atlas ICBM in 1958, NASA with AEC, and especially the Los Alamos Space Laboratories (i.e. LASL), were charged to replace USAF as the ROVER Program Leaders. In 1961 this effort distributed via contracts to Westinghouse and Aerojet General. The industrial branch of ROVER was called under the acronym NERVA (Nuclear Engine for Rocket Vehicle Applications).

The genesis of Project Rover can be traced to 1942, when scientists began to address the idea of using nuclear energy to propel an aircraft or rocket. These ideas were formulated soon after Enrico Fermi and his associates conducted the first successful test of a fission reactor. As early as 1944, scientists at the University of Chicago's Metallurgical Laboratory and Los Alamos began to discuss the possibility of using a fission reactor to heat a gas to high temperatures and propel a rocket, which was essentially the basic idea behind a "nuclear thermal" rocket. These scientists published several reports that explored the potential for this type of rocket.

The reports attracted the attention of the USAF, which actually funded secret, small-scale, studies of nuclear thermal rockets at Oak Ridge, Tennessee at 1946-1949. Interest in nuclear rockets waned until 1954, when Robert Bussard of Oak Ridge Laboratory published a detailed engineering study of several nuclear thermal rocket applications. The Air Force commissioned LASL, Lawrence Livermore National Laboratory and others to perform more theoretical studies of NTR performance.

Early in 1955, Los Alamos summarized its investigations in a report on nuclear powered second stages for intercontinental ballistic missiles. The report touted the performance advantages of nuclear powered rockets, which gathered support for materials research in the field. This report, along with similar information from Lawrence Livermore led to the start of serious nuclear rocket reactor work at both laboratories.

In 1956, Lawrence Livermore was redirected to work on nuclear ramjets, with Los Alamos continuing to develop rockets under Project Rover. As atomic weapons became smaller and lighter, chemical rockets became a viable delivery system. This led USAF, in 1957, to state that nuclear rockets had no longer any military value. Instead USAF recommended that space applications can be pursued.

Project Rover consisted of three principal phases, whose names were from the names of their respective nuclear reactors: the 1st one was Kiwi, which lasted from 1955 to 1964. The 2nd

was Phoebus, which lasted from 1964 to 1969. The last one was Pewee which lasted from 1969 to the project's cancellation at the end of 1972. All nuclear reactors for the Project Rover were assembled at Los Alamos' Pajarito Site. For each engine, there were actually two reactors built, one for "zero-power critical" experiments conducted at Los Alamos and another used for full-power testing at the Nevada Test Site. Fuel and internal engine components for the engines were fabricated in the Sigma complex at Los Alamos.

List of the Nuclear Rocket Engines for Project Rover

- ✚ **Kiwi-A:** Named after the large, flightless bird, Kiwi was the first phase of Project Rover. Kiwi consisted of eight reactors that scientists tested between 1959 and 1964. The first reactor, dubbed Kiwi-A, was fired for the first and last time on July 1, 1959 at the Nevada Test Site.
- ✚ **Kiwi-B:** The Kiwi-B series increased power by ten-fold while maintaining the same size of the Kiwi-A series. The Kiwi-B reactors experienced a problem similar to Kiwi-A: Internal Vibrations caused by dynamic flow instability fractured portions of the fuel elements. Scientists resolved this problem when they developed Kiwi-B4.
- ✚ **Phoebus-1:** During the 1960s, scientists developed the Phoebus series of nuclear reactors to meet the needs of an interplanetary mission, such as a manned mission to Mars. Phoebus-1 was developed to study how best to increase power density. Phoebus A-1 was successfully tested on July 25, 1965.
- ✚ **Phoebus-2:** Scientists increased power density even further with the Phoebus-2 series. However, a limiting factor proved to be the cooling in the aluminum pressure vessel. Despite this limitation, tests run with the Phoebus-2 were considered highly successful. The final Phoebus-2 test in June 1968 ran for more than 12 minutes at 4000 MW (at this time the most powerful nuclear reactor ever built).
- ✚ **Pewee:** Considered as a smaller version of Kiwi. Pewee was fired several times at 500 MW to test coatings made of zirconium carbide. Scientists also increased Pewee's power density. Easy to test and compact. Pewee was ideal for unmanned scientific interplanetary missions.

In Figure 3, there is a direct size comparison of the previous mentioned nuclear engines.

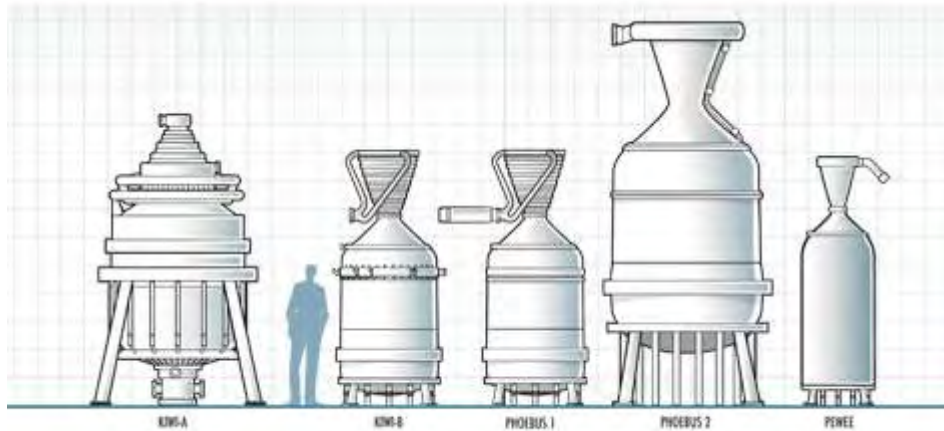


Figure 3: Size comparison of the main series of nuclear rocket engines for Project Rover.

2.2.2 NERVA: Nuclear Engine for Rocket Vehicle Application

In 1961, NASA and the AEC embarked on a second nuclear rocket program known as NERVA. Taking advantage of the knowledge acquired as scientists designed, built and tested Project Rover research reactors, NERVA scientists and engineers worked to develop practical rocket engines that could survive the shock and vibration of a space launch. From 1964 to 1969, Westinghouse Electric Corporation and Aerojet-General Corporation built various NERVA reactors and rocket engines.

In 1969, NERVA's successes prompted NASA's Marshall Space Flight Center director Wernher von Braun to propose sending 12 men to Mars aboard two rockets, each propelled by three NERVA engines. The mission would launch in November 1981 and land on Mars in August 1982.

Although the mission never took place, engines tested during that time, met nearly all of NASA's specifications, including those related to thrust-to-weight ratio, specific impulse, engine restart and engine lifetime. When the Project Rover/NERVA program was canceled in 1972, the only major untested requirement was that a NERVA rocket engine should be able to restart 60 times and operate for a total of 10 hours.

There was one engine, however, that exceeded some NERVA specifications. Designed, built and tested at Los Alamos, the Phoebus-2A Project Rover engine produced up to 4000 MW of thermal power (Figure 4). In those terms, it was the most powerful nuclear propulsion reactor ever built.

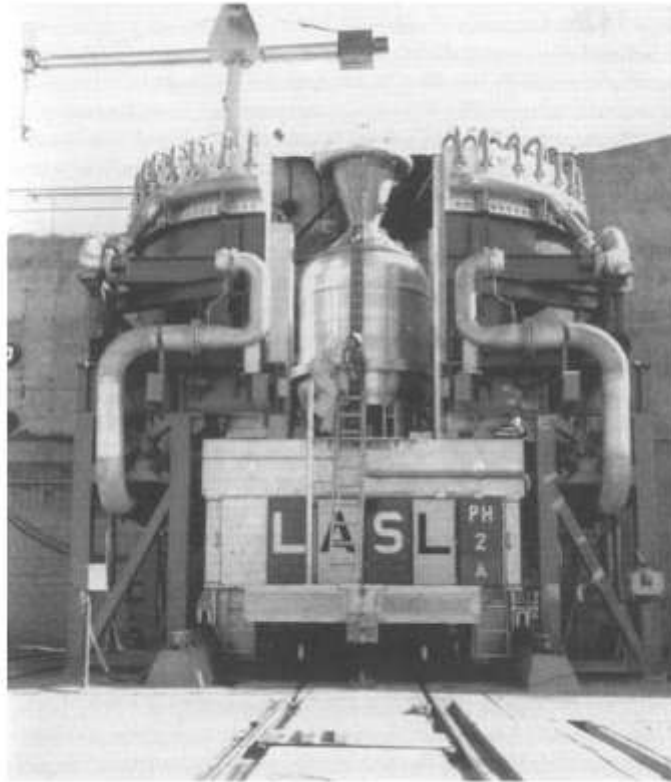


Figure 4: The 4 GW Phoebus-2A nuclear reactor on its test stand at Los Alamos

2.2.3 Nuclear Thermal Rockets

During the Project Rover/NERVA projects, scientists conducted 22 major tests of nuclear thermal rocket engines (Figure 5). Many of these tests explored potential solutions to complex problems that arise when using reactors to propel rockets with hot hydrogen. Significant issues with materials stability, compatibility and corrosion beyond those encountered in terrestrial power reactors had to be addressed to produce practical rockets.

The principal difference between reactors used for space propulsion and electricity generation is the temperature of the cores. The elements of the reactor core are:

1. Fuel elements that contain the radioactive material to produce fission;
2. Structures designed to hold the fuel elements in place;
3. Structures that control the reactor's operation by absorbing, reflecting, or slowing neutrons produced by the fission reactions;
4. A cooling system.

The cooling system (i.e. a working fluid) absorbs heat produced by the fuel elements and transfers the heat or energy to other parts of the system to generate propulsion or electricity.

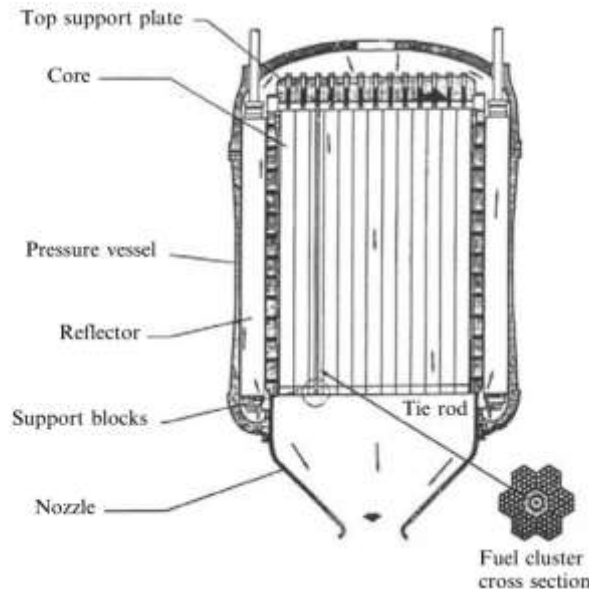


Figure 5: Diagram of a NERVA Kiwi nuclear reactor showing a single fuel bar cross-section

In a nuclear thermal rocket reactor, the temperature must be as high as possible to achieve optimum performance. Thus, the core temperature for the Kiwi-A test was 2683 K, whereas the core of pressurized-water reactors used for nuclear power plants is only around 600 K.

A major difference between a nuclear thermal rocket reactor and a power plant reactor is the cooling systems. Nuclear rockets use hydrogen, whereas US power plants use water. Hydrogen is the best propellant gas for a nuclear thermal rocket.

All the Project Rover/NERVA reactors had solid cores. Researchers designed liquid and gas-core reactors for nuclear thermal rocket propulsion, but only solid-core reactors were built. Few materials, however, remain solid at the temperatures in the core of a nuclear thermal rocket reactor. Structurally, several metals and ceramics with high melting points may be used to build a core, but the way these materials interact with neutrons also plays a key role in their selection.

The first fission reactor consisted of graphite bricks stacked in a pile, with rods of uranium dispersed throughout. Graphite was chosen to build piles mainly because of its good neutronics properties and because it was a weak neutron absorber and a good reflector and moderator of neutrons. However, graphite in a simple pile never encounters the extreme conditions as it would in the core of a nuclear rocket reactor. Graphite's response to these extreme conditions was unknown.

The fuel elements in the cores of the NERVA reactors consisted of uranium-loaded graphite and were utilized using a new method developed by Haskell Sheinberg. Unlike the proven high-temperature method for making graphite parts, the new method worked at room temperature, thus making it easier to fabricate fuel. Also, the new method produced stronger, denser graphite than the traditional method.

The fuel elements in the Kiwi-A core consisted of flat plates molded and pressed at room temperature from a mixture of fine graphite powder called graphite flour, fine carbon powder, graphite flakes, a resin binder and uranium oxide (UO_2) particles.

The extruded fuel elements had a diameter of approximately one inch and were approximately four feet in length. In the early reactors, extruded fuel elements consisted of cylinders with a circular cross-section. Later, the cylinders had the previously mentioned and shown hexagonal cross-section. The number of channels in each fuel element and the channel diameters also changed as reactor designs evolved.

2.2.4 Termination of NERVA Program

NASA's plans for NERVA included a visit to Mars in 1979 and a permanent lunar base by 1981. NERVCA rockets would be used for nuclear "tugs" designed to take payloads from low-Earth orbit to higher, larger orbits as a component of the later-named Space Transportation System. The NERVA rocket would also be used as a nuclear powered upper stage component for the Saturn rocket, which would enable the upgraded Saturn engine to launch much larger payloads to LEO.

In 1973 Project Rover/NERVA was cancelled. Although the projects proved very successful, the space mission itself never took place. No nuclear thermal rockets were ever used to send explorers on long range space missions.

It was the Mars mission that led to NERVA's termination. Members of Congress judged that the manned mission to Mars was too expensive and that funding the project would continue to foster a costly "space race" between the United States and the Soviet Union.

By the time NERVA was cancelled, the NERVA-2 would have met all the mission's objectives. Two of these engines would have been fitted to a NERVA stage capable of powering a manned interplanetary spacecraft.

Despite the cancellation, NERVA engines put some noticeable records:

- 4,500 MW of thermal power
- 3,311 K exhaust temperature
- 250,000 pounds of thrust
- 850 seconds of I_{sp}
- 90 minutes of burn time
- Thrust/Weight equal to $\frac{3}{4}$

2.3 Modern Nuclear Thermal Rocket Concepts

2.3.1 Project Prometheus

In 2000, NASA created Project Prometheus to develop nuclear powered systems for long duration space missions. This project was NASA's most serious consideration of nuclear power for space missions since the cancellation of Project Rover/NERVA in 1972. For the Jupiter Icy Moons Orbiter (JIMO), a spacecraft designed to explore Europa, Ganymede and Callisto, NASA intended to use a Heatpipe Power System reactor, the Project Rover/NERVA's most important spin-off since its cancellation (the Heatpipe Power System reactor is currently the centerpiece of the Los Alamos research program). The JIMO (Figure 6) design used a fission reactor to power a Brayton cycle heat engine that ran an electrical generator. The electricity would then power scientific instruments and an ion propulsion unit. In 2005, NASA canceled the Prometheus Project as a result of budget constraints.



Figure 6: Artistic concept of JIMO reaching Jupiter's moons

2.3.2 Project Bifrost

Project Bifrost is an ambitious study examining emerging space technologies that could lay the foundation for future interstellar flights and investigates the utility of fission for future space missions. The project was initiated by Research Lead Tabitha Smith and Brad Appel working in collaboration with Icarus Interstellar Inc., a nonprofit foundation dedicated to achieving interstellar flight by the year 2100.

2.4 Future of Nuclear Propulsion and other Advanced Concepts

Below, some concepts of possible future propulsion and power systems that could sometime be practical to use, are shown. These systems are explained by terms of propulsion only, but their high energy efficiency is prudent to be used as a power source also.

Nuclear Fission Systems:

- ✚ **Fission Fragment Concept:** It magnetically accelerates the ionized products of nuclear fission as exhaust. It requires no working fluid. The specific acceleration can be from 10^6 seconds. Highly radioactive.
- ✚ **Open-Cycle Gas Core:** It uses a working fluid (LH_2), which is heated through plasma and ejected through nozzle. The exhaust is irradiated and carries fissionable fuel with it, which is harmful. The magnetic containment of plasma is challenging. The specific impulse can be from $3 \cdot 10^3 - 7 \cdot 10^3$ seconds. It can be launched in dormant state.
- ✚ **Closed-Cycle Gas Core:** Here gaseous fission process contained in ablatable transparent vessels (quartz).

Nuclear Fusion Systems:

There are three main types of fusion plasma containment and propulsion concepts.

- ✚ **Magnetic Confinement (MCF):** Here, magnetic fields and magnetic mirrors keep plasma away from walls. Two types of propulsion concepts are the tokamak arrangement or linear device with magnetic mirrors.
- ✚ **Inertial Confinement (ICF):** Here ultra-high-power lasers or particle beams focus plasma into a small region. Some concepts use pellets of fusible material compressed by the beams (pulse fusion). The pellet core can reach temperatures of $100 \cdot 10^6$ K.
- ✚ **Inertial Electrostatic Confinement (IEC):** It is a concept to retain plasma using an electrostatic field. The field accelerates charged particles (like ions or electrons) radially inward, usually in a spherical but sometimes in a cylindrical geometry. Ions can be confined with IEC in order to achieve controlled nuclear fusion.

Various concepts of propulsion are based on the aforementioned types of fusion propulsion concepts. Some of them are the following:

- ✚ **Variable Specific Impulse Magnetoplasma Rocket (VASIMR):** It uses radio waves to ionize and heat a propellant, and magnetic fields to accelerate the resulting plasma to generate thrust. The specific impulse varies with changing the RF heating (dielectric heating) energy, and it can take values between $3 \cdot 10^3 - 3 \cdot 10^4$ seconds.

✚ **Interstellar Ramjet/Bussard Hydrogen Ramjet:** It virtually scoops up interstellar hydrogen for propulsion and power by funneling it into a collector using magnetic fields. The fields must sweep a volume of $10^{18} m^3$ of space to collect 1 gram of hydrogen. It has infinite specific impulse since hydrogen fuel collected in-situ.

Apart from these concepts, some of which are possible to become reality even with contemporary technology and others that will be plausible in the next 50 years, there are some concepts that are only theoretically possible currently.

- ✚ **Matter/Anti-matter Annihilation:** It is possible when two similar, but opposite charge, mass particles collide. They completely converted to energy. It is the highest energy density process in nature; $1 \text{ kg matter} + 1 \text{ kg anti-matter} = 1.8 \cdot 10^{17} \text{ J}$. A M/AM propulsion system could reach up to 10^7 seconds of specific impulse.
- ✚ **Solar Sails:** Use the radiation pressure of a combination of light and high speed ejected gases from a star to push large ultra-thin mirrors to high speeds. Generally, they can provide large specific impulses.
- ✚ **Exotic:** Exist only theoretically. Propellantless concepts, using space-time medium as the energy source. They rely on fluidic space-time, quantum physics, string theory, EM, gravity, Dark Matter/Energy, black holes, gravity waves, alternate dimensions and universal expansion. Highly speculative. Meaningless specific impulse.

Chapter 3

3.1 Brayton Power Systems using Nuclear Reactors

The power systems designed as closed Brayton cycles (CBC) are a common choice for dynamic power conversion for power levels starting from tens of kW and reaching up to thousands of kW, which is a range of power typical for manned spacecraft. Despite this fact, a nuclear heated Brayton cycle power system has never been in space. Although nuclear space power research began with the Systems for Nuclear Auxiliary Power program (SNAP), concurrently with Project Rover/NERVA, the United States sent only one reactor-driven power system in space, which was called SNAP-10.

The SNAP-10 was later followed by SP-100, a joint NASA/DOE venture that ran from 1983 to 1993 and its main focus was to develop a space reactor technology. The SP-100 power system was similar to SNAP-10, in that they both were using thermoelectric conversion with a small reactor. To the other side, the Soviet/Russian space program also used reactors extensively, but their TOPAZ system also used passive thermionic power conversion at relatively low power levels. This system is known as RTG (Radioisotope Thermoelectric Generator).

The first time the nuclear-powered Brayton cycle discussed, was near the end of the Project Rover/NERVA program, when Boman and Gallagher discussed the application of NERVA reactor technology to a Brayton cycle power systems, by using NERVA-derived fuel elements for the heat source of a closed Brayton cycle power system [3]. Up until now, there is an extensive interest for nuclear-powered Brayton cycle power systems, however no actual working systems were utilized. The most recent studies involving the usage of a nuclear powered closed Brayton cycle power system for space applications are Project Prometheus, the Wright et al. work at Sandia National Laboratories and the work at NASA's Glenn Research Center.

3.2 Engine System

The engine system on a Bimodal Nuclear Thermal Rocket consists of two separate thermodynamic cycles, each one being associated with the propulsion and power systems respectively. The cycle that describes the propulsion system is beyond the scope of this thesis and it will only be presented for reasons of clarity. In Figure 7 there is a schematic of the BNTR's engine system, including both cycles. The highlighted area indicates the closed Brayton cycle of the power system.

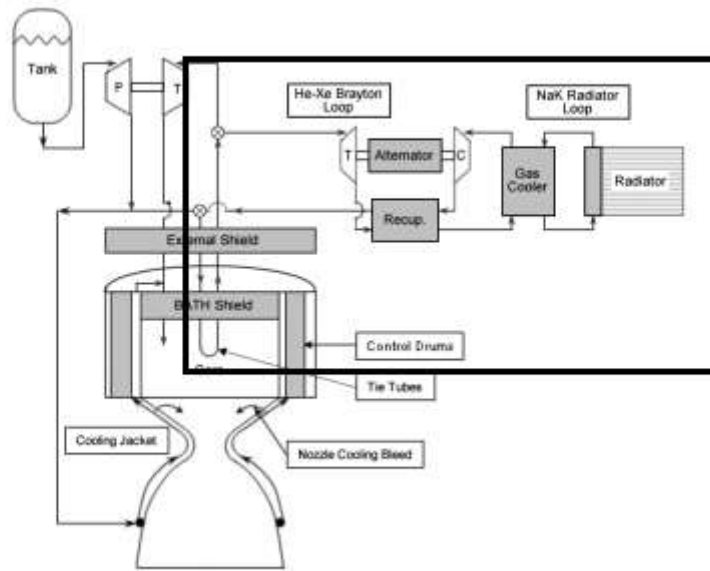


Figure 7: Schematic of the BNTR engine system. The highlighted area represents the power system cycle.

As mentioned before, the nuclear reactor has some support elements which are called tie-tubes and in power generation mode they act as a heat source for the closed Brayton cycle. In propulsion mode the active gas used is hydrogen, whereas in power mode an inert gas-in our case a He-Xe mixture-is used in order to reduce the corrosion of the tie tubes that would occur with hydrogen. From this point, the flow of hydrogen shut off completely, and the only source of active fuel element cooling is the flow of the He-Xe mixture through the tie tubes. Hence, the only common point of the two different thermodynamic cycles is the tie tubes.

As shown in Figure 7, the power generation system is comprised of two separate cycles, the He-Xe Brayton loop and the NaK Radiator loop. The latter is for the cooling of the radiator and it is not of main concern here. The former, however, is the cycle that is analyzed in this thesis.

The Brayton cycle consists of the tie tubes, which will be referred to as the “reactor”, turbine, compressor, recuperator and radiator. The turbine powers the compressor and the alternator (which produces the electrical power) and the recuperator has been added to pre-heats the inlet flow on the reactor, thus improving the cycle efficiency. The waste heat of the cycle is rejected to outer space through the radiator.

3.3 Ideal and Non-ideal Brayton cycles

Below there is an illustration of an ideal (Figure 8) and a non-ideal (Figure 9) Brayton cycle. The purpose of showing both of them is to point the significance of putting a recuperator to the non-ideal cycle for the improvement of the cycle efficiency.

3.3.1 Ideal Brayton cycle

Ignoring irreversibilities as the air circulates through the various components of the Brayton cycle, there are no frictional pressure drops, and the air flows at constant pressure through the heat exchangers. If stray heat transfers to the surroundings are also ignored, the processes through the turbine and compressor are isentropic. Illustrations of an ideal Brayton cycle, along with a temperature-entropy diagram are shown below.

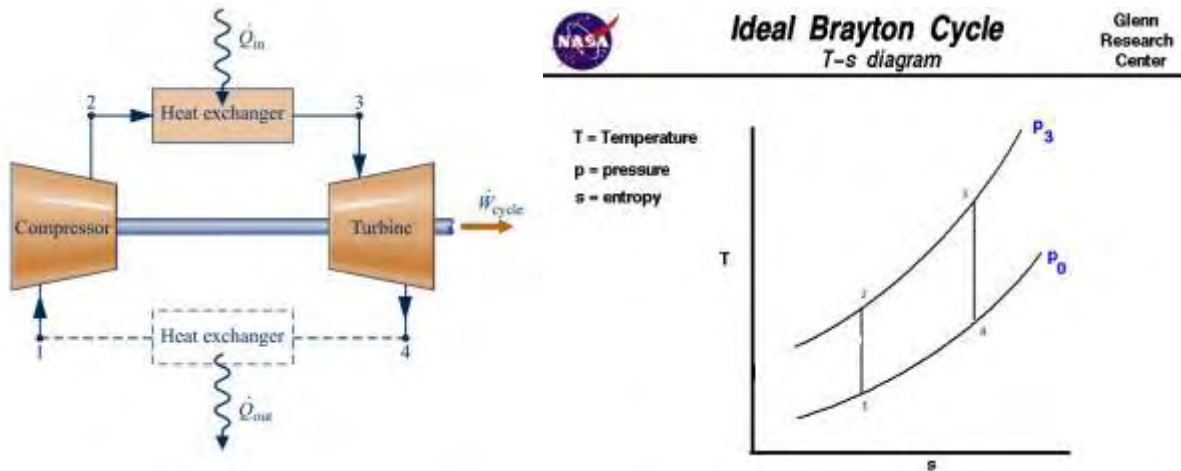


Figure 8: Ideal closed Brayton cycle (left) and a T-s plot (right). [T-s diagram courtesy of NASA]

The ideal Brayton cycle consists of two isobars and two reversible adiabatics (isentropics):

- Air is first compressed reversibly and adiabatically
- Heat is added to it reversibly at constant pressure
- Air expands reversibly, adiabatically in the turbine. The heat is removed from the system reversibly at constant pressure to bring it to original state.

The process on the T-s diagram is as follows:

- 1-2 Isentropic compression
- 2-3 Constant pressure heat addition
- 3-4 Isentropic expansion
- 4-1 Constant pressure heat removal

The thermal efficiency of the ideal Brayton cycle can be written in terms of the temperatures at states 1-4 in the cycle.

$$\eta_{th} = \frac{\dot{W}_{out}}{\dot{Q}_{in}} = 1 - \frac{T_4 - T_1}{T_3 - T_2} \quad \{1\}$$

Since processes 1-2 and 3-4 are isentropic between the same pressures, the temperature ratio across the compressor can be expressed in terms of the pressure ratio. In addition to that, the heat addition at states 2-3 and heat removal at states 4-1 occur at constant pressure. This leads to the relation of the turbine temperature ratio to the compressor temperature ratio.

$$\frac{T_2}{T_1} = \left(\frac{P_2}{P_1}\right)^{\frac{\gamma-1}{\gamma}} = \frac{T_3}{T_4} = \left(\frac{P_3}{P_4}\right)^{\frac{\gamma-1}{\gamma}} \quad \{2\}$$

From the previous equation it can be concluded that $\frac{P_2}{P_1} = \frac{P_3}{P_4} = r_p$ and $\frac{T_4}{T_1} = \frac{T_3}{T_2}$. Using these ratios on equation {2}, new relations can be derived for the temperatures of each state.

$$T_3 = T_4 r_p^{\frac{\gamma-1}{\gamma}} \quad \{3\}$$

$$T_2 = T_1 r_p^{\frac{\gamma-1}{\gamma}} \quad \{4\}$$

$$T_3 - T_2 = (T_4 - T_1) r_p^{\frac{\gamma-1}{\gamma}} \quad \{5\}$$

Substituting equation {5} into {1}, the following equation describing the thermal efficiency occurs.

$$\eta_{th} = 1 - \frac{1}{r_p^{\frac{\gamma-1}{\gamma}}} \quad \{6\}$$

This equation describes the efficiency of an ideal Brayton cycle. The work ratio of the cycle can be easily shown from the equation below.

$$\begin{aligned} \text{Work ratio} &= \frac{mC_p(T_3 - T_4) - mC_p(T_2 - T_1)}{mC_p(T_3 - T_4)} \\ &= 1 - \frac{T_1}{T_3} r_p^{\frac{\gamma-1}{\gamma}} \end{aligned} \quad \{7\}$$

3.3.2 Non Ideal Brayton cycle

The ideal Brayton cycle described above is insufficient for the power generation on a BNTR because it does not take into consideration the use of a recuperator, or the inefficiencies in the compressor, the turbine and the reactor that should have been present in an actual system. Because of frictional effects within the compressor and turbine, the working fluid would experience increases in specific entropy across these components. There would also be pressure drops as the working fluid passes through the heat exchangers.

The turbine exhaust temperature of a single gas turbine is normally well above the ambient temperature. Accordingly, the hot turbine exhaust gas has significant thermodynamic utility (exergy) that would be irrevocably lost due to the gas discarded directly to the surroundings. One way of utilizing this potential is by means of a heat exchanger called a regenerator (in our case the recuperator), which allows the air exiting the compressor to be preheated before entering the combustor, thereby reducing the amount of fuel that must be burned in the combustor. In the case of a regenerated Brayton cycle, the regenerator is a counterflow heat exchanger through which the hot turbine exhaust gas and the cooler air leaving the compressor pass in opposite directions. Ideally, no frictional pressure drop occurs in either stream.

Illustrations of the non-ideal recuperated Brayton cycle, as well as a temperature-entropy diagram are shown below.

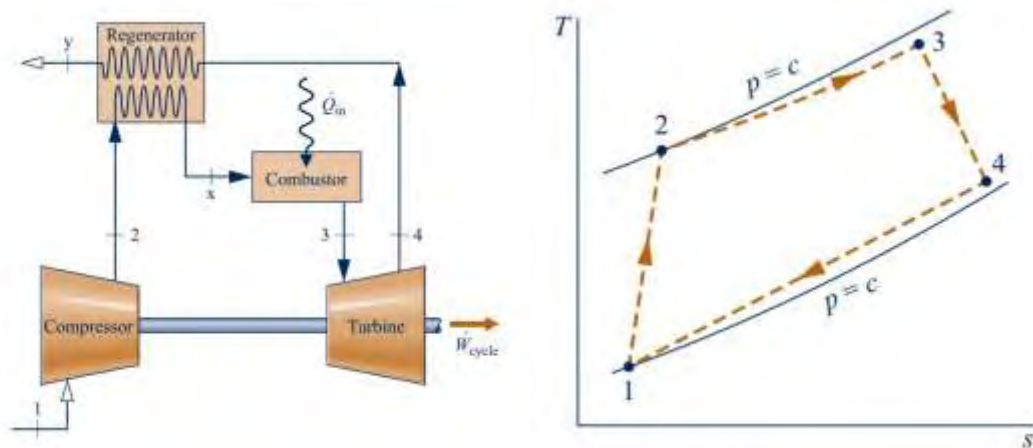


Figure 9: Non ideal recuperated Brayton cycle (left) and T-s plot (right)

The recuperator performance is characterized by its effectiveness, which is expressed as the ratio of the actual heat transfer to the maximum possible.

$$e_R = \frac{h_{2R} - h_2}{h_4 - h_2} \quad \{8\}$$

The isentropic turbine and compressor efficiencies are given by the two following equations.

$$\eta_t = \frac{\left(\frac{\dot{W}_t}{\dot{m}}\right)}{\left(\frac{\dot{W}_t}{\dot{m}}\right)_s} = \frac{h_3 - h_4}{h_3 - h_{4s}} \quad \{9\}$$

$$\eta_c = \frac{\left(\frac{\dot{W}_c}{\dot{m}}\right)_s}{\left(\frac{\dot{W}_c}{\dot{m}}\right)} = \frac{h_{2s} - h_1}{h_2 - h_1} \quad \{10\}$$

The combustion chamber, which in our case is the reactor, has an efficiency defined as the actual enthalpy change resulting from a given input heat transfer.

$$\eta_r = \frac{\dot{m}(h_3 - h_{2R})}{\dot{Q}_{in}} \quad \{11\}$$

3.3.3 Brayton cycle of the Bimodal Nuclear Thermal Rocket

Below there is an illustration (Figure 10) of the Brayton cycle which is utilized in a BNTR, containing all the components mentioned above.

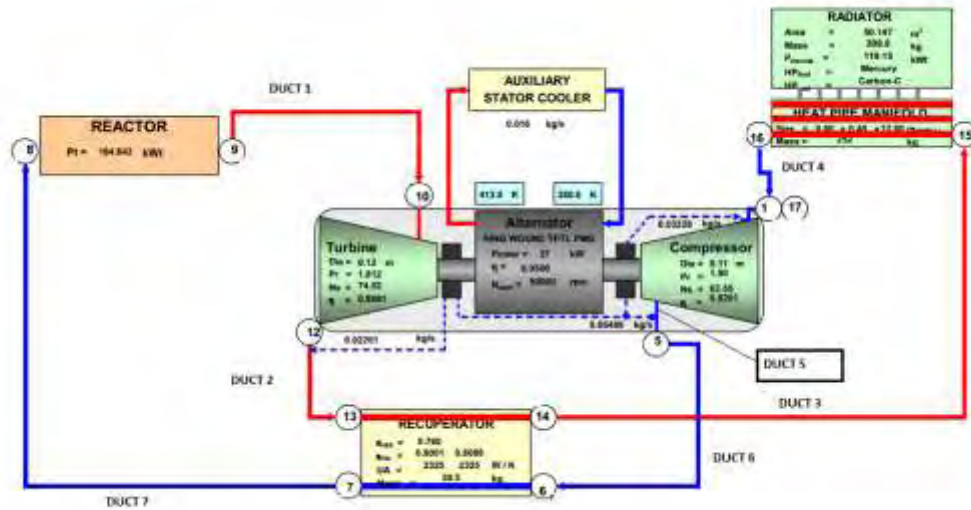


Figure 10: Schematic of the closed Brayton cycle of a BNTR.

In conjunction with the previously mentioned components of the non-ideal recuperated Brayton cycle, the summation of the components, along with few details is presented afterwards:

- ❖ Combustion chamber (reactor): the ^{235}U in the reactor is contained to the tie-tubes. The tie-tubes are made of an UC-ZrC/graphite alloy. A total of 500 of them are contained into the reactor, which corresponds to approximately 10,000 channels. This leads to the conclusion that heat transfer to the propellant is very effective [5]. The reactor is the hot side heat exchanger of the Brayton cycle.
- ❖ Turbine/Compressor: the turbine powers the compressor and the alternator, which produces the electrical power needed.
- ❖ Recuperator: as mentioned before, the recuperator (regenerator) is used to improve the cycle efficiency by pre-heating the reactor inlet flow with the turbine exhaust.
- ❖ Heat Pipe Manifold: it can also be mentioned as a gas cooler. It is essentially the cold side heat exchanger of the Brayton cycle. Its usage is to reject the waste heat from the Brayton cycle to the radiator loop. The hot-leg working fluid is He-Xe whereas the cold-leg is NaK, a liquid metal fluid.
- ❖ Radiator: essential to radiate abundant heat from the cycle to outer space. This happens through a loop between the radiator and the heat pipe manifold. The radiator is not a part of the Brayton cycle, but it is mentioned as a mean of measurement and comparison for the other components of the cycle.
- ❖ 5 major ducts: these ducts, which are mentioned in Figure 10, are connecting the aforementioned components.
 - DUCT 1: it connects the reactor with the turbine.

- DUCT 2: it connects the turbine with the recuperator (hot stream).
- DUCT 3: it connects the recuperator and the heat pipe manifold.
- DUCT 4: it connects the heat pipe manifold with the compressor.
- DUCT 5: it is added to the output of the compressor and before the decrease of the mass flow due to lubrication. The analysis of DUCT 5 was not taken under consideration, since its effects are minor in the final results.
- DUCT 6: it connects the compressor and the recuperator (cold stream).
- DUCT 7: it closes the cycle by connecting the turbine exhaust to the reactor.

The various calculations presented on this thesis were based on the estimations and values presented on the PhD thesis of J. Clough, and they will be presented again on the results section.

In order to calculate the pressure drop across the previously mentioned ducts, and using the numerical results of J. Clough's work, it can be determined that it is proportional to the square power of the flow rate for each one of them.

$$\Delta P = K_p \dot{m}^2 \quad \{12\}$$

Based on this method, the output and input temperatures of the ducts were also calculated.

$$T_{out} = K_T T_{in} \quad \{13\}$$

The He-Xe working fluid is heated in the channels which are located in the reactor. Then, it is led towards the turbine where it is expanded in order to enter to the recuperator and eventually to be cooled through the radiator. After that, the air mixture moves into the compressor so as to be compressed and to be driven again to the recuperator in which is heated up and then re-enter the reactor. It can be seen in Figure 10 that there is an increase and a decrease on the mass flow before the input and after the output of the compressor respectively. There is also an increase of the mass flow in the output of the turbine. The reason of this is for the cooling of the alternator and the lubrication of the shaft.

The temperature of the turbine output is calculated based on {9}.

$$\begin{aligned} \eta_t &= \frac{h_3 - h_4}{h_3 - h_{4s}} && \Rightarrow \\ \eta_t &= \frac{T_3 - T_4}{T_3 - T_{4s}} && \Rightarrow \\ T_4 &= T_3 - \eta_t (T_3 - T_{4s}) && \{14\} \end{aligned}$$

$$\begin{aligned}
\frac{p_{out}}{p_{in}} &= \left(\frac{T_{4s}}{T_3} \right)^{\frac{\gamma-1}{\gamma}} & \Rightarrow \\
\frac{1}{Pr_t} &= \left(\frac{T_{4s}}{T_3} \right)^{\frac{\gamma-1}{\gamma}} & \Rightarrow \\
T_{4s} &= \frac{T_3}{Pr_t^{\frac{\gamma}{\gamma-1}}} & \{15\}
\end{aligned}$$

The pressure ratio of the turbine was initially regarded as 1.812, again using the values from the dissertation of J. Clough.

For the compressor, the output and the isentropic temperatures were calculated using {10} and the ratio of the input and output pressures, which was regarded initially as 1.9.

$$\begin{aligned}
T_{2s} &= T_1 Pr_c^{\frac{\gamma-1}{\gamma}} & \{16\} \\
\eta_c &= \frac{h_{2s} - h_1}{h_2 - h_1} & \Rightarrow \\
\eta_c &= \frac{T_{2s} - T_1}{T_2 - T_1} & \Rightarrow \\
T_2 &= T_1 + \frac{T_{2s} - T_1}{\eta_c} & \{17\}
\end{aligned}$$

The recuperator, including both the hot and the cold stream, and the heat pipe manifold were considered as heat exchangers, so the output pressures were, like the ducts, proportional to the squared power of the mass flow. The coefficient for the calculation of the output temperatures was calculated from the next equation.

$$\frac{\dot{Q}}{\dot{m}CpT_{in}} = K_{T_recuperator} \Rightarrow \frac{UA(T_{out} - T_{in})}{\dot{m}CpT_{in}} = K_{T_recuperator} \quad \{18a\}$$

$$\frac{\dot{Q}}{\dot{m}CpT_{in}} = K_{T_heatpipemanifold} \Rightarrow \frac{\dot{m}Cp(T_{out} - T_{in})}{\dot{m}CpT_{in}} = K_{T_heatpipemanifold} \quad \{18b\}$$

While for the recuperator, it was easy to calculate the temperature coefficient, because of the heat conductance's value that was on the Clough's dissertation, the calculation for the heat conductance coefficient (UA) of the heat pipe manifold was more difficult, but after we obtained

the value of the temperature coefficient, it was much easier. The usage of the heat pipe manifold's heat conductance coefficient will become prominent at the optimization section of this thesis.

For the reactor, there was an assumption that it is both a heat exchanger and a combustion chamber, so the output pressure was directly proportional to the input pressure. This was necessary in order to obtain logical values for our calculations. The output temperature of the working fluid at the reactor was calculated in the next equation.

$$\frac{\dot{Q}}{\dot{m}C_pT_{in}} = K_{T_reactor} \Rightarrow \frac{\dot{m}C_p(T_{out} - T_{in})}{\dot{m}C_pT_{in}} = K_{T_reactor} \quad \{19\}$$

Chapter 4

4.1 Exergy

A very important class of problems in engineering thermodynamics concerns systems or substances that can be modeled as being in equilibrium or stable equilibrium, but there are not in mutual stable equilibrium with the surroundings. The requirements of mutual chemical equilibrium are not met. Any system at a temperature above or below that of the environment is not in mutual stable equilibrium with the environment. In this case the requirements of mutual thermal equilibrium are not met. Any lack of mutual stable equilibrium between a system and the environment can be used to produce shaft work.

Using the second law of thermodynamics, the maximum work that can be produced can be determined. Exergy is a useful quantity that stems from the second law and helps in analyzing energy and other systems and processes.

The exergy of the system is defined as the maximum shaft work that can be done by the composite of the system and a specified reference environment. The reference environment is assumed to be infinite, in equilibrium, and to enclose all other systems. Typically, the environment is specified by stating its temperature, pressure and chemical composition. Exergy is not simply a thermodynamic property, but rather is a property of both a system and the reference environment.

The term exergy comes from the Greek words *ex* and *ergon*, meaning from and work. The exergy of a system can be increased if exergy is input to it.

4.2 Exergy Analysis

Exergy has the characteristic that it is conserved only when all processes occurring in a system and the environment are reversible. Exergy is destroyed whenever an irreversible process occurs. When an exergy analysis is performed on a plant such as power station, a chemical processing plant or a refrigeration facility, the thermodynamic imperfections can be quantified as exergy destructions, which represent losses in energy quality or usefulness. Like energy, exergy can be transferred or transported across the boundary of a system. For each type of energy transfer or transport there is a corresponding exergy transfer or transport.

Exergy analysis takes into account the different thermodynamic values of different energy forms and quantities. The exergy transfer associated with shaft work is equal to the shaft work. The exergy transfer associated with heat transfer, however, depends on the temperature at which it occurs in relation to the temperature of the environment.

The exergy can be defined as “the maximum theoretical work obtainable from an overall system consisting of a system and the environment as the system comes into equilibrium with the environment”.

The exergy concept has five important aspects:

1. Exergy is a measure of the departure of the state of a system from that of the environment. It is therefore an attribute of the system and environment together. Once the environment is specified, a value can be assigned to exergy in terms of property values for the system only, so exergy can be regarded as a property of the system. Exergy is an extensive property.
2. The value of exergy cannot be negative. If a system was at any state other than the dead state, the system would be able to change its condition spontaneously toward the dead state. This tendency would cease when the dead state was reached. No work must be done to effect such a spontaneous change. Accordingly, any change in state of the system to the dead state can be accomplished with at least zero work being developed and thus the maximum work (exergy) cannot be negative.
3. Exergy is not conserved but is destroyed by irreversibilities. A limiting case is when exergy is completely destroyed, as would occur if a system were permitted to undergo a spontaneous change to the dead state with no provision to obtain work. The potential to develop work that existed originally would be completely wasted in such a spontaneous process.
4. Exergy has been viewed thus far as the maximum theoretical work obtainable from an overall system of system plus environment as the system passes from a given state to the dead state. Alternatively, exergy can be regarded as the magnitude of the minimum theoretical work input required to bring the system from the dead state to the given state.
5. When a system is at the dead state, it is in thermal and mechanical equilibrium with the environment, and the value of exergy is zero. More precisely, the thermomechanical contribution to exergy is zero. This contribution to exergy is called chemical exergy. The chemical exergy concept is important in the second law analysis of many types of systems, particularly those involving combustion.

4.3 BNTR Closed Brayton Cycle Exergy Analysis

In order to begin the exergy analysis of the BNTR power mode system, we first have to define the initial state of the cycle shown (Figure 10). Based one more time to J. Clough's work, we consider the output of the reactor (state 8) as the initial state, thus we are using the values for pressure, mass flow and temperature (P_8, \dot{m}_8, T_8 respectively) obtained by J. Clough as the initial values of our system. The ambient temperature was considered 200K (background temperature), the emissivity of the radiator surface equal to 0.9 and the efficiencies of the turbine, the compressor and the alternator equal to 0.9081, 0.8201 and 0.95 respectively.

As mentioned above, the inert gas used in the power mode is a He-Xe mixture. Their relative rate was considered 1:1, meaning that the composition of the mixture is 50-50% of both Helium and Xenon. The specific heat capacity (γ) of the working fluid was 0.34 kJ/kgK.

Their molar chemical exergy is 30.31 and 40.27 kJ/mol respectively [6]. The physical exergy of each state and the chemical exergy were calculated from next equations.

$$Ph_{ex_i} = m_i[h_i - h_0 - T_0(s_i - s_0)] \quad \{20a\}$$

$$Ch_{ex} = \frac{x_{He} \cdot Ch_{ex_{He}} + x_{Xe} \cdot Ch_{ex_{Xe}} + R_{He_Xe} \cdot T_{sink} \cdot (x_{He} \cdot \log(x_{He}) + x_{Xe} \cdot \log(x_{Xe}))}{x_{He} \cdot AB_{He} + x_{Xe} \cdot AB_{Xe}} \quad \{20b\}$$

The total exergy was calculated as the summation of both physical and chemical ones.

$$Ex_{total_i} = Ph_{ex_i} + m_i Ch_{ex_i} \quad \{21\}$$

The “*i*” notation represents the state at which the calculation is made. The enthalpy and the entropy were calculated from equations {22} and {23} respectively. The values for the specific heat C_p and the gas constant R were taken from [7].

$$h_i - h_0 = C_p(T_i - T_0) \quad \{22\}$$

$$s_i - s_0 = C_p \log \frac{T_i}{T_0} - R \log \frac{p_i}{p_0} \quad \{23\}$$

4.4 Works, exergy destruction and exergy efficiency

By utilizing the results obtained from the previous calculations, we proceed to the calculations concerning the works of the turbomachinery parts of the BNTR’s CBC. The works of the compressor, turbine and power generator were calculated from equations {24}, {25} and {26} respectively.

$$P_{compressor} = \dot{m} \Delta h \eta_c \quad \{24\}$$

$$P_{turbine} = \dot{m} \Delta h \eta_t \quad \{25\}$$

$$P_{total} = |P_{compressor} - P_{turbine}| \eta_{alt} \quad \{26\}$$

In equation {25} we use the absolute value of the difference, only in order to demonstrate that the work cannot be of negative value.

As far as the exergy destruction of each process of the closed Brayton cycle, below is a list of the equations necessary to obtain the values of the exergy destruction at the compressor, recuperator, turbine, heat pipe manifold and each duct and they are equations {27}, {28}, {29}, {30}, {31} and {32} respectively. It can be seen that the exergy destruction at the reactor and the heat pipe manifold is been calculated using the same function (using their respective values). This is prudent, in order to show that the reactor and the heat pipe manifold are just the hot and the cold leg of the cycle respectively. This will be proven useful to the optimization section.

$$Ex_destruction_{compressor} = Total_exergy_{input} - Total_exergy_{output} - P_{compressor} \eta_c \quad \{27\}$$

$$Ex_destruction_{recuperator} = Total_exergy_{input(cold)} + Total_exergy_{input(hot)} - Total_exergy_{output(cold)} - Total_exergy_{output(hot)} \quad \{28\}$$

$$Ex_destruction_{reactor} = Total_exergy_{input} - Total_exergy_{output} - (1 - \frac{T_0}{T_{out}}) Q_{reactor} \quad \{29\}$$

$$Ex_destruction_{turbine} = Total_exergy_{input} - Total_exergy_{output} - P_{turbine} \eta_t \quad \{30\}$$

$$Ex_destruction_{heat\ pipemanifold} = Total_exergy_{input} - Total_exergy_{output} - (1 - \frac{T_0}{T_{out}}) Q_{heat\ pipe\ manifold} \quad \{31\}$$

$$Ex_destruction_{duct} = Total_exergy_{input} - Total_exergy_{output} \quad \{32\}$$

The total exergy destruction is the summation of the destructions at each component. Finally, the exergy efficiency of each component and the total exergy efficiency of the system are calculated from the next set of equations.

$$\eta_{exergy_compressor} = \frac{Total_exergy_{output} - Total_exergy_{input}}{P_{compressor}} \quad \{33\}$$

$$\eta_{exergy_turbine} = \frac{P_{turbine}}{Total_exergy_{input} - Total_exergy_{output}} \quad \{34\}$$

$$\eta_{exergy_recuperator} = \frac{Total_exergy_{input(cold)} - Total_exergy_{output(cold)}}{Total_exergy_{input(hot)} - Total_exergy_{output(hot)}} \quad \{35\}$$

$$\eta_{exergy_reactor} = \frac{Total_exergy_{output}}{Total_exergy_{input} + Q_{reactor}} \quad \{36\}$$

$$\eta_{exergy_heatpipemanifold} = \frac{Total_exergy_{output} + Q_{heatpipemanifold}}{Total_exergy_{input}} \quad \{37\}$$

$$\eta_{exergy_total} = \frac{P_{total}}{Q_{reactor}} \quad \{38\}$$

Chapter 5

5.1 Finite Time Thermodynamics

5.1.1 Introduction to Finite Time Thermodynamics

Before we proceed to the exergy optimization of our closed Brayton cycle, an adequate, hopefully, explanation of the process that will be used for the optimization must be mentioned before.

In 1824, Carnot proposed a cycle operating on reversibility principles. In classical thermodynamics the efficiency of a reversible Carnot cycle became the upper bound of thermal efficiency for heat engines that work between the same temperature limits. Thus, when T_H and T_L denote the temperatures of hot and cold thermal reservoirs, thermal efficiency of Carnot cycle for heat engines and the coefficient of performance for refrigerators and heat pumps are expressed $\eta_C = 1 - T_L/T_H$, $COP_{ref,C} = \frac{T_L}{T_H - T_L}$, $COP_{hp,C} = T_H/(T_H - T_L)$ respectively.

But instead of the elegance that the Carnot thermal efficiency and coefficients have, they do not have great significance and are poor guides to the performances of real heat engines, heat pumps and refrigerators. In practice, all thermodynamic processes take place in finite-size devices in finite-time, therefore, it is impossible to meet thermodynamic equilibrium and hence irreversibility conditions between the system and the surroundings. For this reason, the reversible Carnot cycle cannot be considered as a comparison standard for practical heat engines from the view of output rate (power output for a heat engine, cooling load for a refrigerator and heating load for a heat pump) on size perspective, although it gives an upper bound for thermal efficiency.

In order to obtain a certain amount of power with finite-size devices various authors extended the reversible Carnot cycle to an endoreversible Carnot cycle by taking the irreversibility of finite-time heat transfer into account and investigated the maximum power conditions. They obtained the efficiency of an endoreversible Carnot heat engine at maximum power output. However, it should be mentioned and noted that this expression is valid for the heat engines to be designed regarding the maximum power output objective. The proper optimization criteria to be chosen for the optimum design of the heat engines may differ depending on their purposes and working conditions. E.g. for power plants, in which fuel consumption is the main concern, the maximum thermal efficiency criterion is very important, whereas for aerospace vehicles and naval ships, for which propulsion is of great importance, the

maximum power output criterion is significant. On the other hand, for ship propulsion systems, both fuel consumption and thrust gain may be equally important, therefore, in such a case both the maximum power and the maximum thermal efficiency criteria have to be considered in the design. Additionally, size reduction, economical and ecological objectives are considered as other important criteria in the design of real heat engines. In this perspective, many optimization studies for heat engines based on the endoreversible and irreversible models have been carried out in literature by considering essentially finite-time and finite-size constraints for various heat transfer modes.

As a common result of these studies, it can be concluded that the optimal thermal efficiency η_{opt} and optimal power \dot{W}_{opt} for various objectives considering different criteria must be positioned between maximum power and the reversible Carnot heat engine conditions i.e. $\eta_{mp} \leq \eta_{opt} < \eta_C$, $\dot{W}_{max} \geq \dot{W}_{opt} > \dot{W}_C$, where η_{mp} is the thermal efficiency at maximum power \dot{W}_{max} . It must be noted that the Carnot efficiency and the efficiency at maximum power constitute the upper and lower bounds of the thermal efficiency for a given class of heat engines, respectively. It can also be concluded that the efficiency of the reversible Carnot heat engine cycle is the upper limit for the thermal efficiencies of all heat engines whereas the maximized power output of the endoreversible Carnot heat engine is the maximum power limit.

Identifying the performance limits of thermal systems and optimizing thermodynamic process and cycles including finite-time, finite-rate and finite-size constraints, which were called as finite-time thermodynamics (FTT), endoreversible thermodynamics, entropy generation minimization (EGM) or thermodynamic modeling and optimization in physics and engineering literature, have been subject of many books[8].

5.1.2 Optimization of the other heat-engine cycles

In his work, Leff showed that the reversible heat engines (Joule-Brayton, Otto, Diesel and Atkinson) other than the Carnot heat engine operating at maximum work output have efficiencies equal to Chambadal-Novikov-Curzon-Ahlborn, which is also called the thermal efficiency of an endoreversible/irreversible cycle at maximum power output, (CNCA) efficiency although these models involve no finite-time considerations, hence no irreversibilities.

In 1851, James Joule proposed an ‘air engine’ with a piston-cylinder work producing device as a substitute for the widely used steam engine. George Brayton built a piston-driven internal combustion engine based on the same model cycle for about 20 years after Joule’s proposal. However, the efficiency of this circle was about 7%, too low to be competitive. Then the cycle is idealized excluding the air intake and the exhaust parts, incorporating two constant pressure and two isentropic processes. This lead to the ideal model of the Brayton cycle as it is known today [8].

5.1.3 Power density analysis of the closed Brayton cycle

In this thesis the optimization of the closed Brayton cycle for power generation on a Bimodal Nuclear Thermal Rocket is based on the concept of power density analysis. The power density is defined as the ratio of power output to the maximum specific volume in the cycle and it is set as the objective for performance analysis. The same procedure applies on irreversible regenerated closed Brayton cycles coupled to constant-temperature heat reservoirs generally, and it is treated from the viewpoint of finite time thermodynamics (FTT) or entropy generation minimization (EGM) as mentioned previously.

Since the finite time thermodynamics or entropy generation minimization was advanced, much work has been performed on the performance analysis and optimization of finite time processes and finite size devices, as mentioned before. The FTT performance of Brayton cycle has been also analyzed for the power, specific power, efficiency and ecological optimization objectives with the heat transfer irreversibility and/or internal irreversibilities. Sahin *et al* took the power density as the objective function and analyzed the optimum performance of an ideal reversible simple Brayton cycle free of heat transfer and other irreversibilities. Yavuz investigated maximum power density performance for an internally irreversible Brayton cycle free of heat transfer irreversibility. Medina *et al* applied the maximum power density method to an internal irreversible regenerative Brayton cycle free of heat transfer irreversibility, whereas once more Sahin *et al* applied the maximum power density method to an internally irreversible regenerative reheating Brayton cycle free of heat transfer irreversibility. Chen *et al* optimized the distribution of the heat exchanger inventory for maximum power density of a simple endoreversible Brayton cycle coupled to constant-temperature heat reservoirs with the only external heat transfer irreversibility. Furthermore the same research group analyzed maximum power density performance of a simple endoreversible Brayton cycle coupled to variable-temperature heat reservoirs with the only external heat transfer irreversibility. The power density objective was also applied to an endoreversible Carnot heat engine with the only external heat transfer irreversibility, an irreversible Carnot heat engine and a combined cycle Carnot engine with internal irreversibility and external heat transfer irreversibility.

Our approach, based on the work by Chen *et al*, is to analyze the irreversible constant-temperature heat reservoir, regenerated closed Brayton cycle performance using the power density objective with considerations of the heat transfer irreversibility in the hot- and cold-side heat exchangers and the regenerator, the irreversible compression and expansion losses in the compressor and turbine, and the pressure loss in the pipe [9].

Cycle model

We begin our approach by first considering an irreversible regenerated closed Brayton cycle, like the one we have demonstrated in Figure 9, at this time coupled to constant-temperature heat reservoirs, which in our case will be considered the reactor and the heat pipe manifold. This approach is close to reality given the fact that the reactor emits constant temperature due to nuclear fission and the heat pipe manifold is in an external loop with the radiator, so the absorbing temperature will be due to the radiator efficiency. However we can add a slight margin of these values and determine new constant values, even though it is not necessary. The closed Brayton cycle along with the constant-heat temperature is shown in Figure 11.

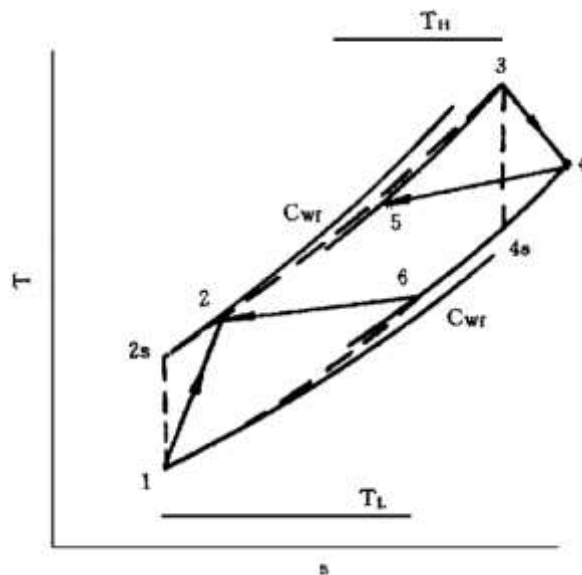


Figure 11: The T-s diagram of an irreversible regenerated Brayton cycle

The heat source temperature is T_H and the heat sink temperature is T_L . Processes 1-2 and 3-4 are non-isentropic adiabatic compression and expansion processes in the compressor and the turbine. Process 2-5 is an isobaric absorbed heat process in the regenerator (recuperator), 4-6 is an isobar-evolved heat process in the regenerator (recuperator). Process 5-3 is an isobar-evolved heat process in the hot-side heat exchanger (reactor) and process 6-1 is an isobar-evolved heat process in the cold-side heat exchanger (heat pipe manifold). Processes 1-2_s and 3-4_s are isentropic and adiabatic, representing the process in an ideal compressor and an ideal turbine. The pressure drop in the piping (ducts) is reflected using pressure recovery coefficients:

$$D_1 = \frac{p_3}{p_2} \quad \{39\}$$

$$D_2 = \frac{p_1}{p_4} \quad \{40\}$$

The irreversibility in the non-isentropic compression and expansion processes is reflected by using the efficiencies of the turbine and the compressor, which were shown in equations {9} and {10} respectively and once again are:

$$\eta_t = \frac{T_3 - T_4}{T_3 - T_{4s}}$$

$$\eta_c = \frac{T_{2s} - T_1}{T_2 - T_1}$$

Let's consider now that we have the irreversible cycle 1-2-3-4. Assuming that the heat exchangers between the working fluid and the heat reservoirs and the regenerator are counter-flow (which is a fact in our case), the heat conductances (heat transfer surface area and heat transfer coefficient product) of the hot- and cold-side heat exchangers (in our case the hot-side heat exchanger is the reactor and the cold-side heat exchanger is the heat pipe manifold) and the regenerator are UA_H, UA_L and UA , and the thermal capacity rate (mass flow rate and specific heat product) of the working fluid is C_{wf} . According to the properties of the heat transfer process, working fluid and heat exchangers, the rate Q_H at which heat is transferred from heat source to working fluid, the rate Q_L at which heat is rejected from the working fluid to the heat sink and the rate Q_R of heat regenerated (recuperated) in the regenerator (recuperator) are given by:

$$Q_H = C_{wf}(T_3 - T_5) = C_{wf}E_H(T_H - T_5) \quad \{41\}$$

$$Q_L = C_{wf}(T_6 - T_1) = C_{wf}E_L(T_6 - T_L) \quad \{42\}$$

$$Q_R = C_{wf}(T_4 - T_6) = C_{wf}(T_5 - T_2) = C_{wf}E_R(T_4 - T_2) \quad \{43\}$$

where E_H, E_L and E_R are, respectively, the effectiveness of the hot- and cold-side heat exchangers and the regenerator and are defined as:

$$E_H = 1 - e^{-N_H} \quad \{44\}$$

$$E_L = 1 - e^{-N_L} \quad \{45\}$$

$$E_R = \frac{N_R}{N_R + 1} \quad \{46\}$$

where N_H , N_L and N_R are the number of heat transfer units of the hot- and cold-side heat exchangers and the regenerator and are defined as:

$$N_H = \frac{UA_H}{C_{wf}} \quad \{47\}$$

$$N_L = \frac{UA_L}{C_{wf}} \quad \{48\}$$

$$N_R = \frac{UA_R}{C_{wf}} \quad \{49\}$$

As again mentioned in Chapter 3, the working fluid isentropic temperature ratio x for the compressor gives:

$$x = \frac{T_2}{T_1} = \left(\frac{P_2}{P_1} \right)^k = \text{Pr}_c^k \quad \{50\}$$

where Pr_c is the compressor pressure ratio and $k=(\gamma-1)/\gamma$, where γ is the ratio of specific heats. According to the definition of the pressure recovery coefficient mentioned in {39}, {40} we have the working fluid isentropic temperature ratio for the turbine as follows:

$$\frac{T_3}{T_4} = \left(\frac{P_3}{P_4} \right)^k = x(D_1 D_2)^k = xD \quad \{51\}$$

where $D = (D_1 D_2)^k$. The power output and the efficiency of the cycle are defined as:

$$W = Q_H - Q_L \quad \{52\}$$

$$\eta = 1 - \frac{Q_L}{Q_H} \quad \{53\}$$

Analytical Relations

From the definition of the compressor and turbine efficiencies we have

$$T_{2s} = (1 - \eta_c)T_1 + \eta_c T_2 \quad \{54\}$$

$$T_4 = (1 - \eta_t)T_3 + \eta_t T_{4s} \quad \{55\}$$

From {41}-{43} the new values for temperature values T_1, T_3, T_5, T_6 we have

$$T_{3_new} = E_H T_H + (1 - E_H)T_5 \quad \{56\}$$

$$T_{1_new} = E_L T_L + (1 - E_L)T_6 \quad \{57\}$$

$$T_{5_new} = E_R T_4 + (1 - E_R)T_2 \quad \{58\}$$

$$T_{6_new} = E_R T_2 + (1 - E_R)T_4 \quad \{59\}$$

From {49}, {50}:

$$T_{2s} = xT_1 \quad \{60\}$$

$$T_{4s} = T_3 x^{-1} D^{-1} \quad \{61\}$$

Substituting {60} into {54} yields:

$$T_{2_new} = \frac{(x - 1 + \eta_c)T_1}{\eta_c} \quad \{62\}$$

Substituting {61} into {55} yields:

$$T_{4_new} = T_3(1 - \eta_t + \eta_t x^{-1} D^{-1}) \quad \{63\}$$

Now, combining {56}, {58} and {63} gives:

$$T_{4_new} = \frac{(1 - \eta_t + \eta_t x^{-1} D^{-1})[E_H T_H + (1 - E_H)(1 - E_R)T_2]}{1 - (1 - \eta_t + \eta_t x^{-1} D^{-1})E_R(1 - E_H)} \quad \{64\}$$

Furthermore, combining {57}, {59} and {64} we have:

$$\begin{aligned} T_{1_new} &= \frac{(1 - E_R)(1 - E_L)(1 - \eta_t + \eta_t x^{-1} D^{-1})E_H T_H}{1 - E_R(1 - \eta_t + \eta_t x^{-1} D^{-1})(1 - E_H)} \\ &+ \frac{[1 - (1 - \eta_t + \eta_t x^{-1} D^{-1})E_R(1 - E_H)]E_L T_L}{1 - E_R(1 - \eta_t + \eta_t x^{-1} D^{-1})(1 - E_H)} \\ &+ \frac{(1 - E_L)[E_R + (1 - E_H)(1 - 2E_R)(1 - \eta_t + \eta_t x^{-1} D^{-1})T_2]}{1 - E_R(1 - \eta_t + \eta_t x^{-1} D^{-1})(1 - E_H)} \end{aligned} \quad \{65\}$$

Solving {62} and {65} gives the final value for T_2 :

$$\begin{aligned} T_{2_new} &= \frac{x - 1 + \eta_c}{G_1} \{ (1 - E_R)(1 - E_L)(1 - \eta_t + \eta_t x^{-1} D^{-1})E_H T_H \\ &+ [1 - (1 - \eta_t + \eta_t x^{-1} D^{-1})E_R(1 - E_H)]E_L T_L \} \end{aligned} \quad \{66\}$$

where

$$\begin{aligned} G_1 &= \eta_c [1 - E_R(1 - E_H)(1 - \eta_t + \eta_t x^{-1} D^{-1})] \\ &- (x - 1 + \eta_c)(1 - E_L)[E_R + (1 - E_H)(1 - 2E_R)(1 - \eta_t + \eta_t x^{-1} D^{-1})] \end{aligned} \quad \{67\}$$

Substituting {67} into {64} gives the final value for T_4 :

$$\begin{aligned} T_{4_new} &= \frac{1 - \eta_t + \eta_t x^{-1} D^{-1}}{G_1} \{ [\eta_c - (x - 1 + \eta_c)E_R(1 - E_L)]E_H T_H \\ &+ (1 - E_R)(1 - E_H)(x - 1 + \eta_c)E_L T_L \} \end{aligned} \quad \{68\}$$

Substituting {66} and {68} into {58} and {59} respectively we take the final values for T_5 and T_6 :

$$T_{5_new} = \frac{1}{G_1} \{ (1 - \eta_t + \eta_t x^{-1} D^{-1}) [E_R \eta_c + (x - 1 + \eta_c)(1 - 2E_R)(1 - E_L)] E_H T_H \quad \{69\}$$

$$+ (x - 1 + \eta_c)(1 - E_R) E_L T_L \}$$

$$T_{6_new} = \frac{1}{G_1} \{ (1 - \eta_t + \eta_t x^{-1} D^{-1})(1 - E_R) \eta_c E_H T_H \quad \{70\}$$

$$+ (x - 1 + \eta_c) [(1 - \eta_t + \eta_t x^{-1} D^{-1})(1 - 2E_R)(1 - E_H) + E_R] E_L T_L \}$$

Substituting {69} into {41} yields:

$$Q_H = \frac{C_{wf} E_H G_2}{G_1} \quad \{71\}$$

Similarly, substituting {70} into {42} yields:

$$Q_L = \frac{C_{wf} E_L G_3}{G_1} \quad \{72\}$$

where

$$G_2 = \{ \eta_c [1 - E_R (1 - \eta_t + \eta_t x^{-1} D^{-1})] - (x - 1 + \eta_c)(1 - E_L) [E_R + (1 - 2E_R)(1 - \eta_t + \eta_t x^{-1} D^{-1})] \} T_H - (x - 1 + \eta_c)(1 - E_R) E_L T_L \quad \{73\}$$

$$G_3 = (1 - \eta_t + \eta_t x^{-1} D^{-1})(1 - E_R) E_H \eta_c T_H - \{ \eta_c [1 - E_R (1 - E_L)(1 - \eta_t + \eta_t x^{-1} D^{-1})] - (x - 1 + \eta_c) [E_R + (1 - \eta_t + \eta_t x^{-1} D^{-1})(1 - 2E_R)(1 - E_H)] \} T_L \quad \{74\}$$

Substituting {71} and {72} into {52} and {53} respectively gives us the dimensionless power output $\bar{W} = W/(C_{wf} T_L)$ and the thermal efficiency η of the cycle in the following manner:

$$\bar{W} = \frac{G_4}{G_5} \quad \{75\}$$

$$\eta = 1 - \frac{G_6}{G_7} \quad \{76\}$$

where $\tau = T_H/T_L$ is the cycle heat reservoir temperature ratio and the coefficients G_4, G_5, G_6, G_7 are as follows:

$$\begin{aligned} G_4 = & \{\eta_c[1 - (1 - \eta_t + \eta_t x^{-1} D^{-1})(E_R + E_H - E_L E_R)] \\ & - (x - 1 + \eta_c)(1 - E_L)[E_R + (1 - 2E_R)(1 - \eta_t + \eta_t x^{-1} D^{-1})]\} E_H \tau \\ & - \{(x - 1 + \eta_c)[E_H(1 - E_R) + E_R + (1 - \eta_t + \eta_t x^{-1} D^{-1})(1 - 2E_R)(1 - E_H)] \\ & - \eta_c[1 - (1 - \eta_t + \eta_t x^{-1} D^{-1})E_R(1 - E_H)]\} E_L \end{aligned} \quad \{77\}$$

$$\begin{aligned} G_5 = & \eta_c[1 - E_R(1 - E_H)(1 - \eta_t + \eta_t x^{-1} D^{-1})] \\ & - (x - 1 + \eta_c)(1 - E_L)[E_R + (1 - E_H)(1 - 2E_R)(1 - \eta_t + \eta_t x^{-1} D^{-1})] \end{aligned} \quad \{78\}$$

$$\begin{aligned} G_6 = & E_L \{(1 - \eta_t + \eta_t x^{-1} D^{-1})(1 - E_R)E_H \eta_c \tau \\ & - \eta_c[1 - E_R(1 - E_H)(1 - \eta_t + \eta_t x^{-1} D^{-1})] \\ & + (x - 1 + \eta_c)[E_R + (1 - \eta_t + \eta_t x^{-1} D^{-1})(1 - 2E_R)(1 - E_H)]\} \end{aligned} \quad \{79\}$$

$$\begin{aligned} G_7 = & E_H \{\{\eta_c[1 - E_R(1 - \eta_t + \eta_t x^{-1} D^{-1})] \\ & - (x - 1 + \eta_c)(1 - E_L)[E_R + (1 - \eta_t + \eta_t x^{-1} D^{-1})(1 - 2E_R)]\} \tau \\ & - (x - 1 + \eta_c)(1 - 2E_R)E_L \end{aligned} \quad \{80\}$$

In addition, due to the ideal gas law we have:

$$p_4 v_4 = RT_4 \quad \{81\}$$

$$p_1 v_1 = RT_1 \quad \{82\}$$

If we now combine {39}, {40}, {81} and {82} we can derive the next relation

$$\frac{v_4}{v_1} = D_2 \frac{T_4}{T_1} = D_2 \frac{T_4}{T_2} \frac{T_2}{T_1} \quad \{83\}$$

which, by using the equations {65}, {66} and {68} transforms into:

$$\frac{v_4}{v_1} = \frac{G_8}{G_9} \quad \{84\}$$

where

$$G_8 = (1 - \eta_t + \eta_t x^{-1} D^{-1}) \{ [\eta_c - (x - 1 + \eta_c) E_R (1 - E_L)] E_H \tau + (1 - E_R)(1 - E_H)(x - 1 + \eta_c) E_L \} \quad \{85\}$$

$$G_9 = \eta_c \{ (1 - E_R)(1 - E_H)(1 - \eta_t + \eta_t x^{-1} D^{-1}) E_H \tau + [1 - (1 - \eta_t + \eta_t x^{-1} D^{-1}) E_R (1 - E_H)] E_L \} \quad \{86\}$$

In conclusion, the power density P_{dens} is defined as

$$P_{dens} = \frac{W}{v_4} \quad \{87\}$$

The dimensionless power density $\bar{P}_{dens} = P / (C_{wf} T_L / v_1)$ is, by using equations {75}, {84} and {87}, calculated as:

$$\bar{P}_{dens} = \bar{W} \frac{v_1}{v_4} = \frac{G_4}{G_5} \frac{G_9}{G_8} \quad \{88\}$$

As we can see from the results, all values, including temperatures, power output and work, can be expressed in terms of the hot- and cold-side heat exchangers and regenerator (recuperator) temperatures and heat conductances, the efficiencies of compressor and turbine, the mass flow rate and the specific heat of the working fluid, all of which have constant values.

Optimum distribution of heat conductance

For the fixed UA_H, UA_L, UA_R , equation {88} shows that there exists an optimum working fluid temperature ratio (x_{opt}) (and a corresponding optimum pressure ratio (π_{opt}), which leads to the maximum dimensionless power density (\bar{P}_{max}). In the practice design, UA_H, UA_L, UA_R are changeable. For a fixed pressure ratio (π), there exists a pair of optimum distributions among the heat conductance of hot- and cold-side heat exchangers and the regenerator for the fixed total heat exchanger inventory, which lead to the optimum dimensionless power density \bar{P}_{max} . The optimum pressure ratio (π_{opt}) leads to the maximum optimum dimensionless power density ($\bar{P}_{max,max}$).

For the fixed hot- and cold-side heat exchanger inventory (UA_T), for the constraint

$$UA_H + UA_L + UA_R = UA_T \quad \{89\}$$

we begin by defining the hot- and cold-side heat conductance distribution u_H and u_L respectively:

$$u_H = UA_H / UA_T \quad \{90\}$$

$$u_L = UA_L / UA_T \quad \{91\}$$

These equations lead to:

$$UA_H = u_H UA_T \quad \{92\}$$

$$UA_L = u_L UA_T \quad \{93\}$$

$$UA_R = (1 - u_L - u_H) UA_T \quad \{94\}$$

We should note that u_H and u_L must satisfy the following conditions:

$$u_H \leq 1 \quad \{95\}$$

$$u_L \leq 1 \quad \{96\}$$

$$u_H + u_L \leq 1 \quad \{97\}$$

The point of these constraints is that if $u_H + u_L = 1$, then the regenerated Brayton cycle becomes a simple one (without regeneration). If $u_H + u_L \geq 1$, then practically this cycle does not exist [10]. As we will see to the Results chapter, these constraints are satisfied.

Chapter 6

Results

Thermodynamics & Exergy

In this chapter, the numerical results of the exergy analysis and optimization for the power mode of a Bimodal Nuclear Thermal Rocket will be presented. The software used for the calculations was the Mathworks MATLAB 7.12 (R2011a). For the calculations, a sufficient code was developed to demonstrate, for each state of the closed Brayton cycle, the values of temperature, pressure, mass flow and physical and total exergy. Furthermore, the values of heat emission and work consumption for each component of the cycle are demonstrated, as well as the exergy destruction and efficiency of the components. Finally the results from the exergy optimization are demonstrated.

In order to begin the simulation of the cycle, a presentation of the initial values used is necessary.

TABLE 1

<u>Constants</u>	<u>Values</u>
C_p	0.34 kJ/Kg s
$(\gamma - 1) / \gamma$	0.4
π_t	1.812
π_c	1.9
T_{sink}	200 K
η_t	0.9081
η_c	0.8201
UA	2.325 kW/K
η_{alt}	0.95
Ch_{exHe}	30.31 kJ/mol
Ch_{exXe}	40.27 kJ/mol
x_{He}	50%
x_{Xe}	50%
R_{He-Xe}	0.136 kJ/mol
AB_{He}	0.004 kg/mol
AB_{Xe}	0.131 kg/mol

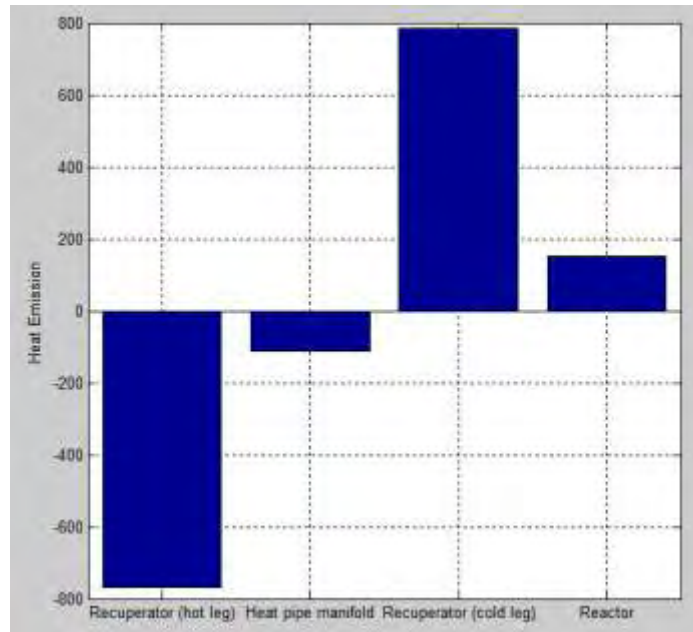
<i>Initial Temperature</i>	911.81 K
<i>Initial Pressure</i>	1023.97 kPa
<i>Initial Mass Flow</i>	1.201 kg/s

The values of temperature, pressure and mass flow for each state of the cycle are presented in Table 2. We began the analysis from State 8, which in our cycle is the output of the reactor.

TABLE 2

<u>State</u>	<u>Temperature [K]</u>	<u>Pressure [kPa]</u>	<u>Mass Flow [kg/s]</u>
8	911.810	1023.970	1.201
9	1284.000	1018.290	1.201
10	1280.280	1015.060	1.201
12	1034.250	560.188	1.224
13	1022.177	557.949	1.224
14	691.046	557.949	1.224
15	691.046	557.919	1.224
16	426.156	546.806	1.224
1	426.156	544.997	1.256
17	426.156	544.998	1.224
5	578.260	1035.495	1.201
6	578.260	1033.305	1.201
7	915.81	1030.915	1.201

The values of heat emission and absorption of each component is presented in the next graph



As we can see in the case of the hot leg of the recuperator and the heat pipe manifold, there is a negative value of Q , which is prudent since there is a temperature drop to their outputs. The “lost” heat is absorbed by the cold leg of the recuperator and the separate cycle of the heat pipe manifold and radiator respectively. In the cold leg of the recuperator there is the absorption of the lost heat from the cold leg of the recuperator. The reactor is playing, as mentioned before, the combustion chamber of the cycle. The exact values are:

- $Q_{recuperator (hot leg)} = -769.879435 \text{ kJ/s}$
- $Q_{heat pipe manifold} = -110.226443 \text{ kJ/s}$
- $Q_{recuperator (cold leg)} = 784.692351 \text{ kJ/s}$
- $Q_{reactor} = 151.980064 \text{ kJ/s}$

The works of the compressor and the turbine are the following:

- $P_{turbine} = 91.231908 \text{ kW}$
- $P_{compressor} = 53.257175 \text{ kW}$

The total work from the power generator of the cycle is the following:

- $P = 36.075996 \text{ kW}$

The physical exergy of each state is presented in Table 3 below:

TABLE 3

State	Physical Exergy [KW]
9	366.596694
10	366.596694
12	365.210834
13	267.702742
14	263.524463
15	158.338476
16	158.336688
17	87.674049
1	87.563781
5	89.873793
6	146.800965
7	144.088126
8	144.018964

The chemical exergy of the He/Xe mixture in the cycle is:

- $E_{chemical} = 243.502173$ kJ/mol

The total exergy of each state is presented in Table 4 below:

TABLE 4

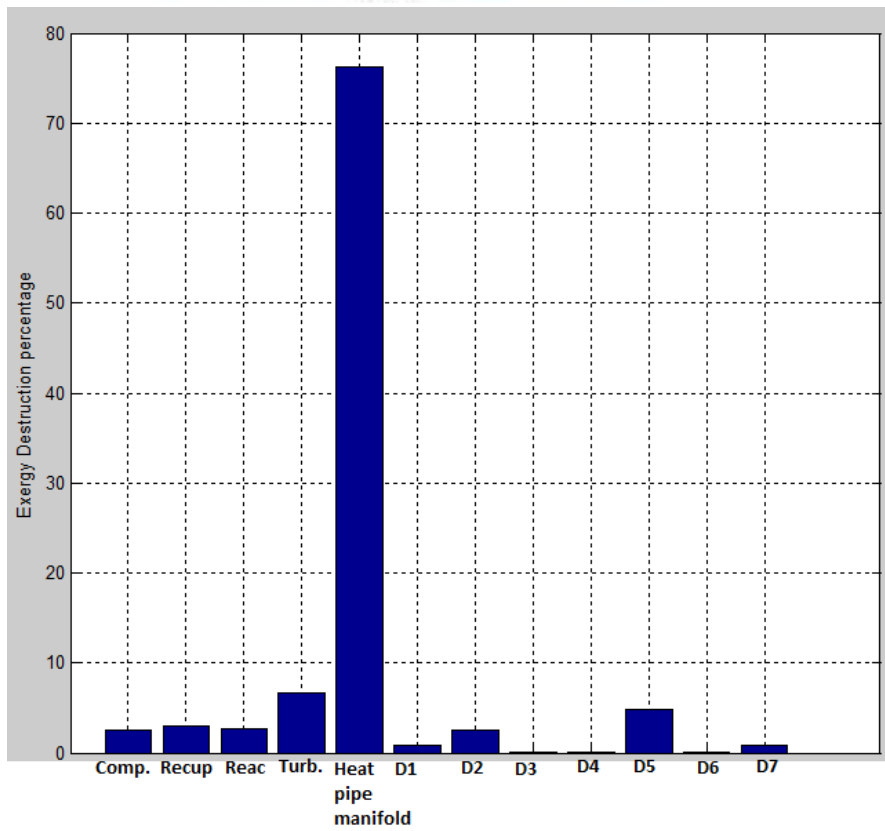
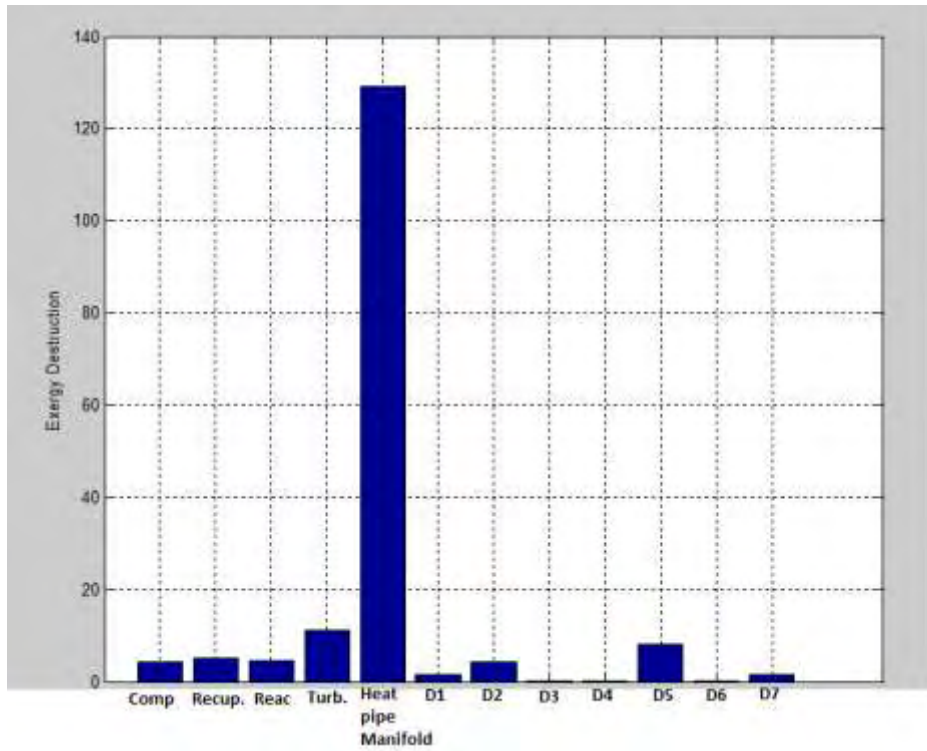
State	Total Exergy [KW]
9	659.042804
10	659.042804
12	657.656944
13	565.654436
14	561.476157

15	456.290170
16	456.288382
17	385.626230
1	385.515962
5	395.686224
6	444.753147
7	436.534236
8	436.465074

The values of the exergy destruction and the percentage of it for each component of the cycle (including the ducts) are presented in Table 5 below:

TABLE 5

Component	Exergy destruction [kW]	Exergy destruction percentage [%]
Compressor	12.408	7.323
Turbine	11.222	6.623
Recuperator	4.976	2.936
Heat pipe manifold	129.131	76.208
Reactor	4.464	2.634
DUCT1	1.385	0.817
DUCT2	4.178	2.465
DUCT3	0.002	0.001
DUCT4	0.110	0.065
DUCT5	0.000	0.000
DUCT6	0.069	0.040
DUCT7	1.496	0.883
Total exergy destruction	169.445	100.00



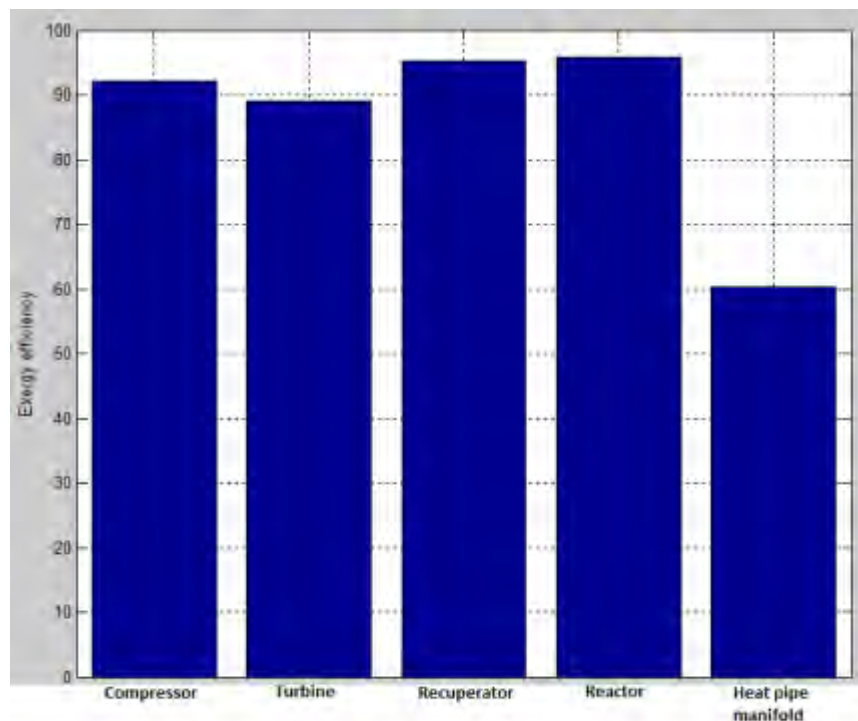
It is obvious that the greater percentage of exergy destruction is at the heat pipe manifold. The reason for this is that the heat pipe manifold directs most of its energy (in the form of heat) to the radiator, and from there to outer space, leading to a big loss of energy and consequently to a big exergy destruction.

The total system exergy efficiency is presented below:

- *System Exergy Efficiency* = 23.737321%

The exergy efficiency of each component of the cycle is presented below:

- *Compressor Exergy Efficiency* = 92.132040
- *Turbine Exergy Efficiency* = 89.046065
- *Recuperator Exergy Efficiency* = 95.250593
- *Reactor Exergy Efficiency* = 95.905441
- *Heat Pipe Manifold Exergy Efficiency* = 60.356520



The lower value of the heat pipe manifold's exergy efficiency is again explained due to the heavy loss of heat at this component, due to its connection to the radiator.

Optimization

The results obtained from the optimization due to the finite-time thermodynamics described in the previous chapter are presented below.

Firstly, the initial values used for the necessary calculations are presented.

Heat conductances (hot & cold side heat exchangers)	Value [kW/K]
• $UA_{hot} (Input\ Massflow * C_p)$	0.4083
• $UA_{cold} (m_{15} * C_p)$	0.4160

Thermal capacity rate	
• C_{wf_hot}	0.4083
• C_{wf_cold}	0.4160
• $C_{wf_recuperator}$	0.4083

The dimensionless power output and the thermal efficiency of the cycle are the following:

- $\bar{W} = 0.1952$
- $\eta = 0.6829$

The power density and the dimensionless power density are the following:

- $P = 34.8497\ kW / m^3$
- $\bar{P} = 0.1177$

For an eager researcher, some parts of the MATLAB code that was developed is presented in the Annex of this thesis, which can be used in order to obtain more thorough results concerning the various constants and variables that are presented.

Concerning the optimization section, there is not any previous research on the specific topic of the power mode of a Bimodal Nuclear Thermal Rocket, so there are no previous results that we can compare with. This should be another issue for any future researcher in the topic of optimization for a closed Brayton cycle for space power systems.

CONCLUSIONS

The purpose of this thesis was a first-of-its-kind demonstration of the exergy analysis and optimization of the power mode of a Bimodal Nuclear Thermal Rocket. The power mode is demonstrated as a closed Brayton cycle, which uses the nuclear reactor of the rocket as a heat capacitor. The cycle was separated into multiple sections, each one representing a state of the cycle. Using initial values concerning pressure ratios, temperatures, mass flows and efficiencies obtained from the Ph.D. dissertation of J. Clough, as long as values necessary for the calculation of the chemical exergies of the cycle's working fluid (He-Xe mixture), an exergy analysis containing exergy destruction and efficiency of the cycle of the power mode was obtained.

Finally, a first numerical approach of the optimization of a closed Brayton cycle for space applications by using the finite-time thermodynamics (or entropy generation minimization) process was obtained. The results are considered satisfactory, but since this is a first approach, further study concerning the issue of optimization may be mandatory.

For future modeling of a closed Brayton cycle for space power systems, an adequate research concerning the modeling of performance maps for both the compressor and the turbine (relations between mass flow, pressure ratios and efficiencies) with the use of analytical functions should be pursued. This research is mandatory in order to determine the function performance of these components.

It is also prudent to state that research on the various aspects of nuclear space propulsion and power generation must continue further concerning the whole concept of the Bimodal Nuclear Thermal Rocketry, which is the most promising, up until now, technology that could lead humankind to the far reaches of our Solar system and establish constant presence there. With the ongoing improvement of the various parts contained to the rocket, new studies must be done, that will ultimately lead to better and better results. One other thing that researchers must pay attention to is that with the improvement of technology, very soon humankind will experience the benefits of nuclear fusion. This will lead to a whole new generation of nuclear space propulsion and power generation concepts, a generation that will eventually take humankind to the stars. So it is imperative that the research on these concepts must keep the pacing on the next decades.

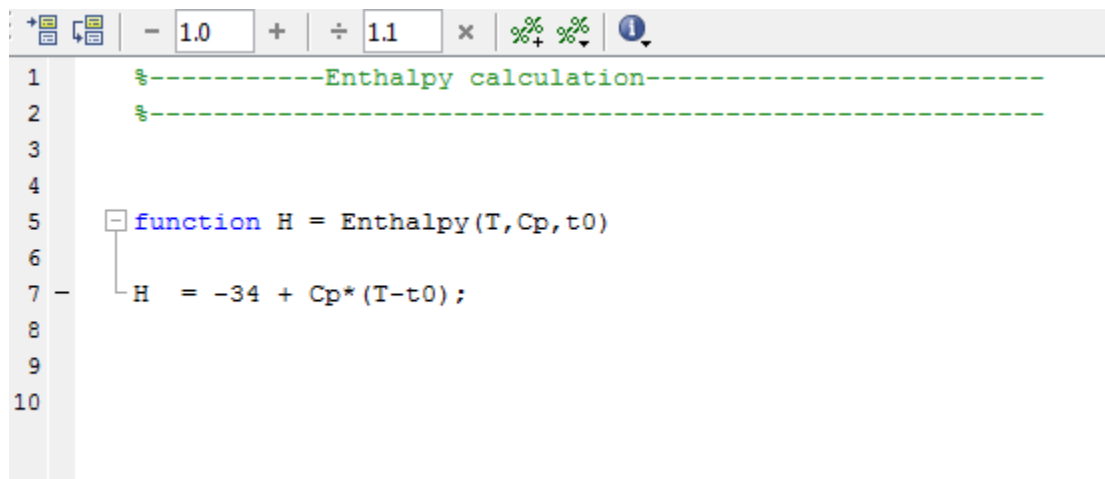
Annex

MATLAB code

In this section, a brief presentation of the MATLAB code that was developed for calculation of the different values of this thesis will be presented. It must be mentioned, though, that only parts of the code, as long as the functions for the entropy, enthalpy and physical exergy, will be presented here. The numericals that thoroughly described in the previous chapters are adequate enough for future research.

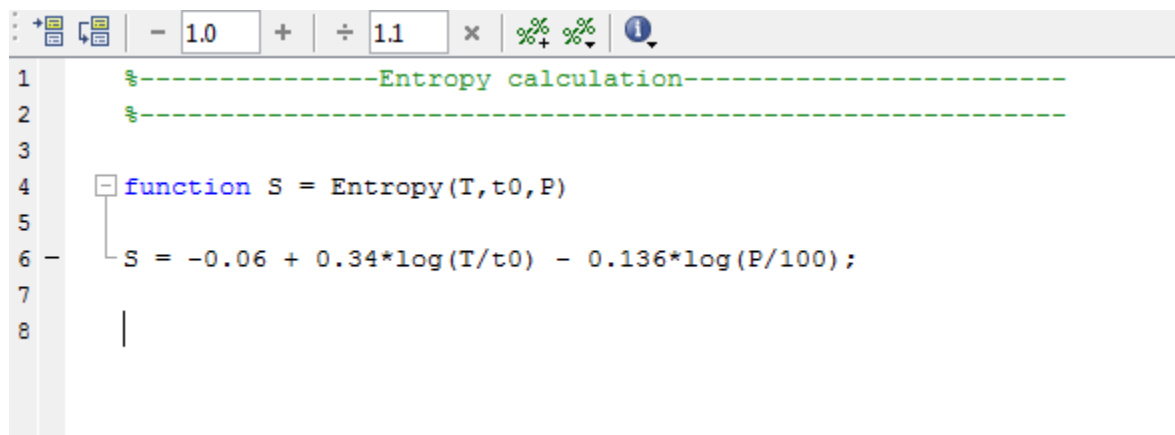
1. Supplemental Functions

Enthalpy calculation:



```
1 %-----Enthalpy calculation-----  
2 %-----  
3  
4  
5 function H = Enthalpy(T,Cp,t0)  
6  
7 H = -34 + Cp*(T-t0);  
8  
9  
10
```

Entropy calculation:



```
1 %-----Entropy calculation-----  
2 %-----  
3  
4 function S = Entropy(T,t0,P)  
5  
6 S = -0.06 + 0.34*log(T/t0) - 0.136*log(P/100);  
7  
8 |
```


Physical Exergy:

```
1 %-----Exergy calculation-----  
2 %-----  
3  
4 function E_ph = Exergy_ph(m,h,s,h0,s0,t0)  
5  
6 E_ph = m*(h-h0-t0*(s-s0)); %kW
```

2. Main code

Here, as mentioned before, only parts of the code will be presented. Specifically, for the initial state, both inlet variables and the initialization are presented, as well as States 8, 9 (Reactor), States 1, 2 (Compressor), States 11, 12 (Turbine) and States 7, 8, 13, 14 (Recuperator, both legs).

Reactor:

```
%-----STATE 8 REACTOR-----  
  
T8 = Inlet_Temp;  
P8 = Inlet_Press;  
m8 = Inlet_Massflow;  
s8 = Entropy(T8,T0,P8);  
h8 = Enthalpy(T8,Cp,T0);  
E_ph8 = Exergy_ph(m8,h8,s8,h0,s0,T0);  
E_total8 = E_ph8 + m8*E_ch; %kW  
  
%-----STATE 9 REACTOR-----  
  
T9 = Inlet_Temp*(KT_reactor + 1);  
P9 = Inlet_Press*KP_reactor;  
m9 = Inlet_Massflow;  
h9 = Enthalpy(T9,Cp,T0);  
s9 = Entropy(T9,T0,P9);  
E_ph9 = Exergy_ph(m9,h9,s9,h0,s0,T0);  
E_total9 = E_ph9 + m9*E_ch;
```

Compressor:

```
§-----STATE 1 COMPRESSOR-----  
  
T1 = T17;  
P1 = P17;  
m1 = Inlet_Massflow+0.022612+0.03228;  
h1 = Enthalpy(T1,Cp,T0);  
s1 = Entropy(T1,T0,P1);  
E_ph1 = Exergy_ph(m1,h1,s1,h0,s0,T0);  
E_total1 = E_ph1 + m1*E_ch;
```

```
§-----STATE 2 COMPRESSOR-----  
  
T2_is = T1*Prc^ex_g;  
T2 = T1+(T2_is-T1)/nc;  
P2 = P1*Prc;  
m2 = Inlet_Massflow+0.022612;§+0.03228;  
h2 = Enthalpy(T2,Cp,T0);  
s2 = Entropy(T2,T0,P2);  
E_ph2 = Exergy_ph(m2,h2,s2,h0,s0,T0);  
E_total2 = E_ph2 + m2*E_ch;
```

Turbine:

```
§-----STATE 11-----  
  
T11_is = T10/(Prt^ex_g);  
T11 = T10 - nt*(T10 - T11_is);  
P11 = P10/Prt;  
m11 = Inlet_Massflow;  
h11 = Enthalpy(T11,Cp,T0);  
s11 = Entropy(T11,T0,P11);  
E_ph11 = Exergy_ph(m11,h11,s11,h0,s0,T0);  
E_total11 = E_ph11 + m11*E_ch;
```

```
§-----STATE 12-----  
  
T12 = T11;  
P12 = P11;  
m12 = Inlet_Massflow + 0.02261;  
h12 = Enthalpy(T12,Cp,T0);  
s12 = Entropy(T12,T0,P12);  
E_ph12 = Exergy_ph(m12,h12,s12,h0,s0,T0);  
E_total12 = E_ph12 + m12*E_ch;
```

Recuperator:

- Cold Leg

```
%-----STATE 13-----
```

```
T13 = KT_12_13*T12;  
P13 = P12 + KP_12_13*(Inlet_Massflow + 0.02261)^2;  
m13 = Inlet_Massflow + 0.02261;  
h13 = Enthalpy(T13,Cp,T0);  
s13 = Entropy(T13,T0,P13);  
E_ph13 = Exergy_ph(m13,h13,s13,h0,s0,T0);  
E_total13 = E_ph13 + m13*E_ch;
```

```
%-----STATE 14 RECUPERATOR-----
```

```
T14 = T13 + (1/UA)*KT_13_14*(Inlet_Massflow + 0.02261)*Cp*T13;  
P14 = P13;  
m14 = Inlet_Massflow + 0.02261;  
h14 = Enthalpy(T14,Cp,T0);  
s14 = Entropy(T14,T0,P14);  
E_ph14 = Exergy_ph(m14,h14,s14,h0,s0,T0);  
E_total14 = E_ph14 + m14*E_ch;
```

- Hot Leg

```
%-----STATE 7 RECUPERATOR-----
```

```
T7 = T6+(1/UA)*KT_6_7*Inlet_Massflow*Cp*T6;  
P7 = P6+KP_6_7*Inlet_Massflow^2;  
m7 = Inlet_Massflow;  
h7 = Enthalpy(T7,Cp,T0);  
s7 = Entropy(T7,T0,P7);  
E_ph7 = Exergy_ph(m7,h7,s7,h0,s0,T0);  
E_total7 = E_ph7 + m7*E_ch;
```

```

%-----STATE 8_pre RECUPERATOR-----

T8_pre = T7+KI_7_8*T7;
P8_pre = P7+ KP_7_8*Inlet_Massflow^2;
m8_pre = Inlet_Massflow;
h8_pre = Enthalpy(T8_pre,Cp,T0);
s8_pre = Entropy(T8_pre,T0,P8_pre);
E_ph8_pre = Exergy_ph(m8_pre,h8_pre,s8_pre,h0,s0,T0);
E_total8_pre = E_ph8_pre + m8_pre*E_ch;

```

The rest of the code can be implied from the equations presented in previous chapters.

REFERENCES

Cited Papers

- [1] The Vision for Space Exploration, NASA, Washington D.C., February 2004.
- [2] Thornton, G. "Introduction to nuclear propulsion- introduction and background lecture 1, Feb. 26-28, 1963". Nuclear Materials Propulsion Operation. NASA Technical Report Server.
- [3]"NERVA Technology Reactor Integrated with NASA Lewis Brayton Cycle Space Power Systems", Journal of Spacecraft and Rockets, Vol. 8, No. 5, May 1971, pp. 500-505.
- [4]"Prometheus Project Final Report" Tech. Rep. 982-R120461, NASA Jet Propulsion Laboratory, Pasadena, CA, October 2005.
- [5]F. P. Durham, "Nuclear Engine Definition Study Preliminary Report ", Engine Description Tech. Rep. LA-5044-MS, Los Alamos Scientific Laboratory, Los Alamos, NM, 1972, vol.1.
- [6]R. Rivero, M. Garfias, Standard Chemical Exergy Of Elements updated,(2006) Energy Vol. 31, Issue 15, pp. 3310–3326.
- [7]J. Tarlecki, N. Lior, N. Zhang, “Analysis of thermal cycles and working fluids for Power generation in space”, Energy Conversion & Management, 48 (2007), pp. 2864–2878.
- [8] A. Durmayaz, O.S. Sogut, B. Sahin, H. Yavuz, “Optimization of thermal systems based on finite-time thermodynamics and thermoeconomics”, Progress in Energy and Combustion Science, 30(2004), pp.175-217.
- [9] L. Chen, J. Zheng, F. Sun, C. Wu, “Power Density Analysis for a Regenerated Closed Brayton Cycle”, Open Sys. & Information Dyn., 8(2001), pp. 377-391.
- [10]L. Chen, J. Zheng, F. Sun, C. Wu, “Power Density Optimization for an Irreversible Regenerated Closed Brayton Cycle”, Physica Scripta, 64(2001), 184-191.

Bibliography

Integrated Propulsion and Power Modeling for Bimodal Nuclear Thermal Rocket, J. Clough, 2007, PhD Dissertation.

Deep Space Propulsion: A roadmap to Interstellar Flight, K.F. Long, 2012, ISBN: 978-1461406068.

Buttler, Tony; Gordon, Yefim (2004), Soviet secret projects: Bombers since 1945. Hinckley: Midland Publications. ISBN: 1-85780-194-6.

Rocket and Spacecraft Propulsion: Principles, Practice and New Developments, Martin J. L. Turner, 3rd edition, 2008, ISBN: 978-3540692027.

Future Spacecraft Propulsion Systems Enabling Technologies for Space Exploration, Paul A. Czysz, Claudio Bruno, 2nd edition, 2009, ISBN: 978-3540888130.

Fundamentals of Engineering Thermodynamics, Michael J. Moran, Howard N. Shapiro, 7th edition, 2011, ISBN: 978-0471274711.

EXERGY: Energy, Environment and Sustainable Development, Ibrahim Dincer, Marc A. Rosen, 1st edition, 2007, ISBN: 978-0080445298.

Internet Sources

www.lanl.gov/science/NSS/issue1_2011/story4full.shtml

news.discovery.com

<https://wiki.ucl.ac.uk/display/MechEngThermodyn/Gas+Power+Cycles>

